POLITECNICO DI MILANO

School of Industrial and Information Engineering

Master of Science in Automation and Control Engineering

POLITECNICO
MILANO 1863

CoKitting: an online scheduling algorithm for human-robot kitting collaboration

Supervisor: Prof. Paolo ROCCO

Co-supervisor: Riccardo MADERNA

Author:

Matteo Poggiali ID: 862704

Academic Year: 2018 – 2019

To my family

Contents

List of Figures

List of Tables

Abstract

With a wide variety of products in the assembly line, it is necessary to supply the components through kitting operations, which consists of creating a set of parts to be sent to the assembly lines. This challenging logistical task is frequently performed manually by warehousemen. The work of taking the objects is often light but implies a great repetitiveness in arm movement. Workers perceive work as repetitive and have some physically stressful working situations that can lead to work-related musculoskeletal disorders.

This thesis proposes a collaborative approach to kitting operations, i.e. some parts are collected by the warehouseman while others are picked by the robot. More specifically, an online scheduling algorithm has been developed that improves the cycle time of the overall system and reduces worker's effort when assembling the kit. The algorithm generates tasks schedule in real-time and sends information to the robot and human about the object to be taken. The ergonomics information is provided by a function obtained offline with the help of Kinect and the REBA method. Finally, the new solution was tested in realistic experimental human-robot kitting system.

Keywords: Robotics, human-robot collaboration, kitting, optimization, scheduling

Sommario

Le linee di assemblaggio presentano grandi varietà di prodotti; ciò rende necessario fornire i componenti attraverso operazioni di kitting, che consistono nel creare un insieme di parti da inviare alla linea di assemblaggio. Questo compito, logisticamente complesso, viene solitamente assolto da operai. Pur non essendo un lavoro fisicamente dispendioso, prevede una gran ripetitività di movimenti delle braccia, e viene quindi percepito come stressante dai lavoratori. Questi fattori possono portare al sorgere di disturbi muscoloscheletrici.

Questa tesi illustra un approccio al kitting collaborativo nel quale alcune parti che compongono il kit vengono prese dall'operaio mentre altre sono prese dal robot. In particolare, è stato sviluppato un algoritmo di scheduling online che diminuisce il tempo di preparazione del kit e al contempo riduce lo sforzo fisico percepito dall'operaio durante l'assemblaggio dello stesso. L'algoritmo genera un piano dei compiti in tempo reale e invia informazioni agli agenti circa quale oggetto debba essere preso. Le informazioni riguardo l'ergonomia di ogni azione di picking vengono fornite all'algoritmo da una funzione ottenuta offline combinando il metodo REBA e il Kinect. Infine, la nuova soluzione è stata testata in un sistema di kitting sperimentale.

Parole chiave: Robotica, collaborazione umano robot, kitting, ottimizzazione, schedulazione

Chapter 1

Introduction

Parts feeding in Just-In-Time(JIT) mixed-model assembly lines, i.e. where distinct models of a product are assembled in the same assembly line, is a challenging operation due to the variety of components needed by each end product (EP) assembled on the line. Among line feeding modes studied in the literature (e.g. line stocking, sequencing and kitting), sequencing and kitting seem to be the most frequently used (especially in the automotive and electronics industry). The reason is that they reduce congestion at the border of the line, which is the area parallel to the assembly line where parts are stored. Kitting consists of preparing, for each EP in the production sequence, a collection or a 'kit' of parts ready for use by assembly operators. Thus, a 'traveling kit' is a kit associated with an EP and moves with it to feed several workstations, while a 'stationary kit' holds parts needed for several EPs and is used by a given workstation until depletion. Parts that form a kit are physically placed together in one or more compartmented containers referred to as 'kitting boxes'. Figure 1.1 shows an example of manual kitting.

Despite the advantages of kitting, there is a great need to improve present picking systems in terms of their efficiency. The physical exposure of workers must also be considered when improvements are made in picking systems since work-related musculoskeletal disorders are common in manual

materials handling that generally involves repetitive movements and work postures with the arms abducted and elevated. These work conditions are known risk factors, especially for neck and upper limb disorders. A possible solution can be an investment in automated kitting systems using robot manipulators.

However, despite the advances in robotics and bin picking applications, actual tests carried out in the field reveal that robotic picking still faces some limitations: for example, the robot cannot pick complex parts. Moreover, kitting requires placing an important variety of parts into the corresponding narrow compartments of a kitting box, which is considered as a complex task in the case of a robotic kitting system because parts need to be precisely positioned. This leads to the development of a hybrid robot–operator kitting system where both a robot and an operator are involved in kit preparation.

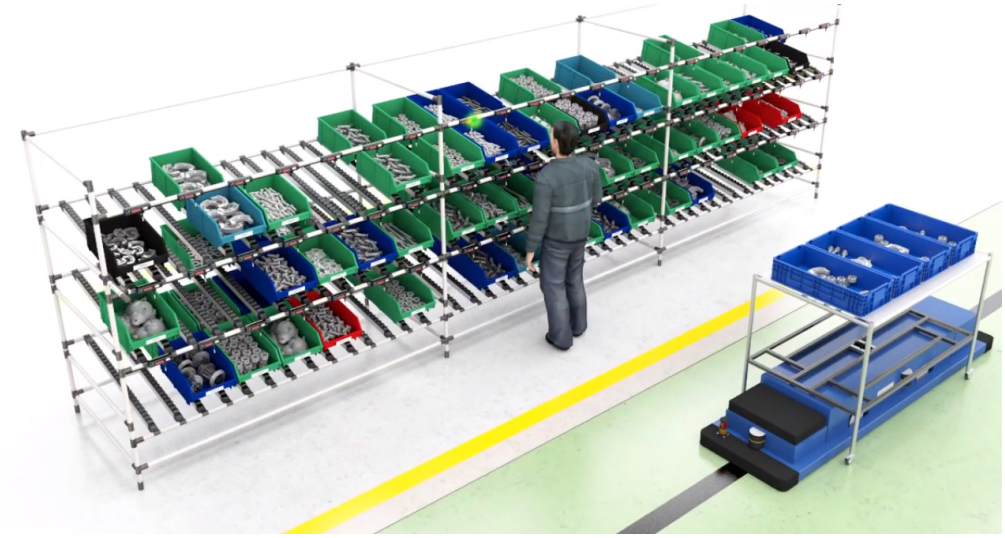

Figure 1.1: Example of manual kitting performed by a warehouseman.

1.1 Thesis objectives

This thesis aims to propose a solution the efficient human-robot kitting collaboration. Although there are some works about collaborative kitting, they mainly focus on the robot and in particular on the visual recognition of objects, in the correct grip and positioning of the object, or on the increase of the process efficiency alone. Production time and efficiency have often been used as criteria for assessing the performance of manufacturing teams, but worker ergonomics for a given job must also be taken into account. Injuries resulting from repetitive movements and excessive fatigue of the operator should be prevented by distributing the work in a manner that reduces his/her physical stress. This thesis jointly considers time and ergonomics to develop a human-robot kitting system where the two agents work in a shared environment. The result is an online scheduler that allocates work between a single human worker and a single robot while reducing production makespan (kit completion time) and physical strain. To estimate the human physical stress, an ergonomic function has been defined that returns a score based on the weight and height of the object to be picked and the height of the worker. The algorithm was then implemented in a real system with the industrial robot Comau Smart Six, simulating an industrial kitting process, to validate the algorithm and verify its improvements. The results obtained through this online scheduler algorithm are an increase of the process productivity compared to the baseline case, i.e. where the kit is assembled by the human worker, and even compared to an offline scheduler and a general improvement in the process ergonomics.

1.2 Chapters organization

The remainder of this thesis work is organized as follows:

The second chapter gives an overview of the state of the art, in partic-

ular about autonomous and collaborative kitting solutions.

The third chapter presents the solution adopted to estimate the human worker physical strain in the kitting process. The reasons for the adopted method are discussed, together with the details of the experiment conducted to develop the ergonomic function.

The fourth chapter describes the proposed MILP (mixed-integer linear programming) solution adopted in order to realize the human-robot kitting collaboration. It presents the adopted constraints and shows a scheduling example.

The fifth chapter shows the results of simulations and experiments with the aim of validating the scheduling algorithm and verifying performance.

The last chapter concludes of the whole thesis, analyzing objectives given the experimental results. Moreover, it proposes possible future work and developments.

Chapter 2

State Of The Art

This chapter aims to give a brief overview of the state of the art of related topics before going into details of the human-robot kitting collaboration proposed in this thesis. Hence, a literature survey regarding autonomous and cooperative kitting is presented in the following.

2.1 Kitting

Most of the existing literature on kitting is related to the problem of choosing the best feeding mode, for each component, among kitting and other line feeding modes such as line stocking and sequencing, see [14]. Sequencing is a particular form of stationary kit where only one part reference, i.e. the variants of a specific component, is carried per kit. In contrast with kitting and sequencing, line stocked parts are supplied to the assembly workstations in boxes where each box contains several pieces of the same variant. Issues on ergonomics and time efficiency in kitting environments have also been addressed: in [10] the authors show the impact of several factors on picking time, including packaging type and size, angle of exposure of storage bins (the use of gravity flow racks allows for angled bins), the height of storage racks and part size.

In contrast, there is limited research regarding robotic kitting systems,

most of which deal with technical aspects related to robotics, vision and grasping tools. Design factors and criteria to implement an effective robotic system are discussed in [26], while performance evaluation of robotic kitting systems can be found in [24], where the authors assess various robotic configurations in terms of throughput, the average time a kit spends in the system and robot utilization. In [16] and [6] a robotic system for automotive kitting within the STAMINA project is proposed. The large mobile manipulation robot consists of an industrial manipulator mounted on a heavy automated guided vehicle platform, capable of pick parts from the Kitting supermarket and bring them to the assembly line. The system utilizes the software control platform SkiROS for high-level control of the mission, which is composed of skills. Each skill solves a specific sub-task: i.e. detecting the part, generating a grasp, etc. One unresolved issue with the above systems is that due to a large number of different objects, a large variety of grasps is required to safely manipulate them. Moreover, kitting requires placing an important variety of parts into the corresponding narrow compartments of a kitting box, which is considered as a complex task in the case of a robotic kitting system because parts need to be precisely positioned. In [2] and [19], these problems have been addressed by introducing a hybrid kitting system. [2] investigate the introduction of a robot into the kitting process, developing a mathematical model that optimally assigns stock keeping units to either the robot or the operator so that the cycle time of the overall system is optimized. The system is designed so that humans and robots do not work in the same space but each in their kitting supermarket. [19] instead presents a mobile manipulation robotic system for collaborative kitting with fast arm trajectory replanning, which can work in the same human environment, but as [16] and [6] it focuses on the part recognition and placement in the box. On the contrary, this thesis focuses more on the effective coordination between humans and robots in the kitting operations.

Research on the allocation of manufacturing tasks to humans and robots

has focused mainly on determining and minimize safety risks, although more recent work has considered the ergonomic benefits of the integration of robots into task plans for human workers. [27] proposed a method for task planning in a hybrid assembly cell which includes both human and robot, based on multi-criteria, such as average resource utilization, mean flow time and ergonomics. [9] described an approach for considering ergonomics as well as human movement capability to ascertain the optimal assembly sequences for human-robot collaboration. They considered cognitive and physical properties as well as functional-allocation criteria that minimized ergonomically poor work conditions while minimizing the number of human-robot changes in the workflow. Execution time between assembly steps allocated to the human and the robot utilized the predetermined motion time system: the human assembly time is estimated by analyzing the motion elements of the assembly while the robot assembly time is determined by simulating the robot movements. Ergonomic factors were based on a linear combination of the OWAS (Ovako Working Posture Analysis System) [1], however, this method is limited to categorize common postures. [20] presents an interesting optimization-based approach that utilizes hierarchical modeling to quantify physical stress in assembly operations and generates human-robot task plans exploring the trade-offs between ergonomics and productivity. They formulated the problem of assigning works between human and robot as mixed-integer linear programming (MILP). However, they do not account for spatial limitations i.e. spatial constraints. Kitting requires a choreography of human and robot work that meets temporal constraint and spatial restrictions on agent proximity to support safe and efficient human-robot co-work.

Chapter 3

Ergonomic Measurement

One of the aims of this thesis is to improve the physical exertion of the manual kitting process that presents repeated arm movements, handling, and lifting of material. According to the Sixth European Working Conditions Survey [8], these remain common issues in working condition. Taking into account worker's health and also welfare costs, it is mandatory to apply policies aimed at minimizing risks belonging to the work-related musculoskeletal disorders (WMSDs). WMSDs includes all musculoskeletal disorders that are induced or aggravated by work and the circumstances of its performance.

Ergonomic factors are increasingly taken into account when designing kitting stations as in [25] where a study is carried out at a Volvo plant in Sweden that analyzes the use of 3D CAD systems to increase the efficiency and ergonomics of a kitting station, thus seeking a reduction in physical exertion through the workspace redesign. In [4] a study on a new method of kitting is presented: the traditional piker-to-material method is replaced with the material-to-picker approach. In the traditional one, kitting is done in a storage area where a material picker moves him/herself between material containers (storage packages) pick parts and put them into the kit box. Conversely, in the second approach, storage packages are moved to material pickers, reducing the need for transportation. In this study,

efficiency and ergonomics of the process are analyzed, showing an increase in productivity, through this new approach does not correspond to an increase in the fatigue perceived by the worker. Despite this, the picking work is still repetitive and stressful in some situations for the worker. The best applicable practice to prevent WMSDs consists in the evaluation of exposure to risk factors in the workplace and the planning of eventual ergonomic inventions such as the workplace redesign, see [25] and [4]. Many methods have been developed with this goal. They can be classified into three groups: self-report, direct measurement and observational methods. Self-reports methods suffer from non-objective factors and are affected by intrinsic limits of subjective evaluations. Direct methods, used for example in [4] and [25], use data from sensors attached to the worker's body, but they are typically more expensive, intrusive, and time-consuming. Observational methods consist of directly observing the worker and the corresponding tasks to estimate the physical exertion. These methods are widely applied in industry and easy to use, so this last method has been chosen as the best one for our application.

Many observational methods have been developed to estimate the physical exposure of tasks in the industry. A detailed review of the most common observational methods can be found in [1]. In industrial practice, posture data are collected through subjective observation or estimation of body-joint angles in pictures/videos, and field expert performs ergonomic analysis. In recent years, however, there have been many studies on the use of low-cost and calibration-free depth cameras, such as the Microsoft Kinect sensor to collect postural data at high frequencies, simplify ergonomic evaluations and allow online assessment. Not all observational methods are suitable for automatic assessment. Among them, the most used one is the RULA method (Rapid Upper Limb Assessment) [18], that gives a score based on the angles of upper body joints and object weights. In [12] the authors describe a framework combining the Kinect v1 skeleton tracking feature with the RULA method for 3D motion analysis. [21] presented an

interesting study on the validation of RULA grand-scores obtained using Kinect v2 data, both in the laboratory and real workplace conditions. [17] presented K2RULA, a semi-automatic RULA evaluation software based on Microsoft Kinect v2, aimed at detecting potential WRMS postures in real-time, however, they tested their tool in a laboratory set-up and not in a real working environment where objects can occlude the hands, as in [21]. Since the kitting process does not involve the upper part, but the whole body, we rely on a different technique, similar to RULA, which consider the complete posture to assess the physical exertion for an operation. This technique, called REBA (Rapid Entire Body Assessment) [13], is well-accepted un industry and suitable for automatic online assessment. Although the REBA technique has been initially developed for pen-paper observations, the fact that it handles static as well as dynamic postures and that it relies on quantitative values makes it suitable for an automatic assessment as the RULA technique. The scheduling algorithm developed in this thesis distributes the objects to be taken to form the kit among the human worker and the robot. Therefore there is a need to associate each picking action with a physical effort score. For that reason, an ergonomic function was implemented using Microsoft Kinect v2, which takes as input the position and weight of the object to be taken from the rack plus the human worker height, and assigns a physical effort score to the object. This score is the REBA score associated with the picking action. In particular, for the physical strain estimation, only the movement of picking the object from the rack is considered, instead of the complete movement involved in the kitting process. This is done given the study carried out in [4], which demonstrates the picking motion to be the most stressful and tiring part of the whole process of kitting.

In the following, Section 3.1 details the REBA method, Section 3.2 shows the experimental procedure used to collect the REBA data. Finally, in Section 3.3 a comparison between the experimental physical effort score and the estimated one is reported.

3.1 REBA Method

The REBA method consists in the fulfillment of an assessment grid, where the human body is divided into two sections:

i) **Section A**, which considers trunk, legs and neck position, plus a correction that accounts for the force load on the limbs.

ii) **Section B**, which considers lower arm, upper arm, and wrist position.

A score is associated with each of these sections using two tables. Finally, a third table takes as input the previous section scores and returns an intermediate score. The REBA grand-score is obtained summing this intermediate score with the activity score, that accounts for the repetitiveness of the action considered. An action level list indicates the severity of the ergonomic risk associated with the task and the intervention required to reduce the risks of injury of the operation:

- 1 grand-score: negligible risk, no action required
- 2-3 grand-score: low risk, change may be needed
- 4-7 grand-score: medium risk, further investigation, change soon
- 8-10 grand-score: high risk, investigate and implement change
- 11+ grand-score: very risk, implement change

Further details on the calculation of REBA score are given in the Appendix A.

In the following, it is shown how the REBA score, for Kitting physical strain estimation purpose, can be seen, as well as a function of the object weight, as a function of the object height position and human worker height instead of body joint angles.

The REBA score C can be formulated as follows:

$$C = C(\underline{\vartheta}, \underline{\varphi}, w) = C(A(\underline{\vartheta}, w), B(\underline{\varphi})) \tag{3.1}$$

where A and B are the values obtained from the two respective sections. The A score is a function of the object weight w and the joint angles of trunk, legs and neck $\underline{\vartheta}$, while the B score is a function of the joint angles φ of the arm that performs the picking operation. Moreover, A is the sum of two functions, one depending on the body joint position $\underline{\vartheta}$ and one depending on the weight w:

$$A(\underline{\vartheta}, w) = A'(\underline{\vartheta}) + A''(w)$$

so C can be written as:

$$C(\underline{\vartheta}, \underline{\varphi}, w) = C(A'(\underline{\vartheta}) + A''(w), B(\underline{\varphi}))$$

Since kitting operations consists of taking objects from a rack, for the same person the body joints angles will depend on the object height position, while two people differ in height will take different postures to reach the same object. For instance, the taller one will find it easier to take objects placed at the top, while it will find more difficult to take those at the bottom. The opposite holds for the shorter people. Therefore, the score A and B are expected to be a function of the object and worker heights, h_o and h_w, respectively. We can thus write:

$$C(A(\underline{\vartheta}, w), B(\underline{\varphi})) = C(A(h_w, h_o, w), B(h_w, h_o))$$

Therefore the REBA score C for a single picking action can be expressed as:

$$C = C(h_w, h_o, w) = C(A'(h_w, h_o) + A''(w), B(h_w, h_o)) \tag{3.2}$$

where $A''(w)$ is already fully defined and $A'(h_w, h_o)$ and $B(h_w, h_o)$ can be identified collecting picking data for different height position of the object and people height. Therefore the ergonomic estimator function $\hat{C}$ it's the result of the identification of C. For simplicity of notation the REBA score without object weight score A'' is indicated as $C_0 = C(h_w, h_o, 0)$. In the following of how data was collected to build the $\hat{C}$ function is explained.

(a) Microsoft Kinect v2 sensor. **(b)** Sensors location on Kinect v2.

Figure 3.1: Image of the Microsoft Kinect v2 sensor (a) and scheme of sensors location (b).

3.2 Ergonomic Function Identification

For the ergonomic function identification and so for the retrieval of the A' and B functions, it has been used the Microsoft Kinect v2 device (see Fig. 3.1a). Inside its case, a Kinect sensor contains(see Fig. 3.1b):

- An RGB camera that stores three-channel data (one per color) in a 1920x1080 resolution
- An infra-red (IR) emitter and an IR depth sensor with a resolution of 512x424 for both IR and depth image acquisition.
- A multi-array microphone, which contains four microphones for capturing sound. The presence of multiple microphones allows to record audio as well as to find the location of the sound source.

Moreover, Microsoft Kinect has an integrated tracking algorithm that returns a hierarchical skeleton composed of joint objects (see Fig. 3.2). Each joint position is calculated in real-time as the average of positions stored in a 300 ms memory buffer (about 10 valid frames at 30 Hz) to minimize jittering. If the sensor is not able to track a joint (e.g. occlusion), its position is inferred (inferred joints) from the surrounding joints by the Kinect SDK.

To evaluate the REBA score 23 of the 25 tracked joints are required. This is one of the reasons to prefer the use of an ergonomics function instead of an online physical exertion tracking: since so many joint positions are required to calculate the REBA score, any disturbance due to self-occlusions or object-occlusions can significantly degrade measurement. The next section reports how the reference frames for evaluating the REBA angles are built.

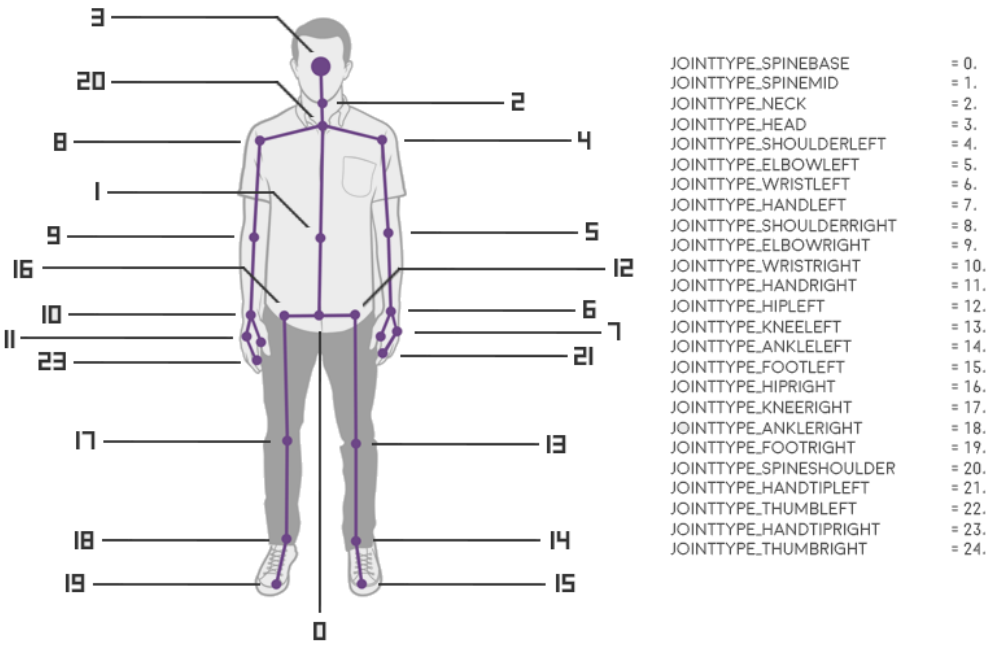

Figure 3.2: Joint positions with respect to the body returned by the Kinect algorithm.

3.2.1 Reference Frames

As in [21] and [7], some reference frames are defined to extract the REBA angles, which are defined in the following:

- *the global coordinate frame* (GCF): Z-axis is along the trunk axis represented by the vector from the spine base (0 in Fig. 3.2) to the

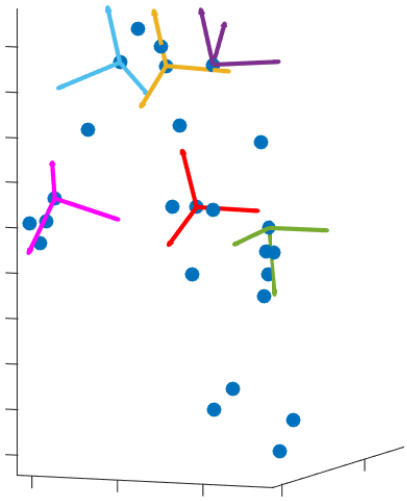

Figure 3.3: Body coordinate frames: red GCF, yellow TCF, violet LSCF, light blue RSCF, green RWCF, magenta LWCF. The blue dots are the body joints.

spine shoulder (20 in Fig. 3.2). The Y-axis is defined as the normal of the plane formed by the Z-axis, the left (12 in Fig. 3.2) and the right (10 in Fig. 3.2) hips. Finally, the X-axis is computed as the normal of the X-axis and the Y-axis. The origin of this frame is the spine base joint.

- *trunk coordinate frame* (TCF): Z-axis is represented by the vector from the spine mid (1 in Fig. 3.2) to the spine shoulder joint (20 in Fig. 3.2). The X-axis is defined as the normal of the plane formed by the Z-axis, the left (4 in Fig. 3.2) and the right (8 in Fig. 3.2) shoulder. Finally, the X-axis is computed as the normal of the Z-axis and Y-axis. The origin of this frame is the spine shoulder joint.

- *right shoulder coordinate frame* (RSCF): Z-axis is the same vector of the trunk coordinate frame. The X-axis is represented by the

projection of the vector from the right shoulder (8 in Fig. 3.2) to the right elbow (9 in Fig. 3.2) into the plane passing through the right shoulder and orthogonal to the Z-axis. The Y-axes is the normal of the Z-axis and X-axis. The origin of this frame is the right shoulder joint. The *left shoulder coordinate frame* (LSCF) is computed similarly.

- *right wrist coordinate frame* (RWCF): X-axis is represented by the vector from the right elbow (9 in Fig. 3.2) to the right wrist (10 in Fig. 3.2). The Y-axis is defined as the vector belonging to the plane passing through the right wrist (10 in Fig. 3.2), right thumb (24 in Fig. 3.2) and the right-hand tip (23 in Fig. 3.2) and, finally, the Z-axis is computed as the normal of the X-axis and Y-axis. The origin of this frame is placed on the right shoulder joint. The *left wrist coordinate frame* (LWCF) is computed in a similar way.

The resulting frames are shown in Fig. 3.3, where red represents the GCF, yellow the TCF, violet and light blue the LSCF and RSCF, green and magenta the LWCF and RWCF and the blue dots are the tracked body joints.

3.2.2 REBA Angles Computation

This section explains how the body positions required in the REBA assessment grid are calculated based on the data returned by the Kinect tracking algorithm. The body positions needed to compute the REBA and how they were obtained are illustrated below:

- The *neck flexion/extension* is assessed computing the angle between the TCF Z-axis and the projection of the vector from the shoulder spine (20 in Fig. 3.2) to the head (3 in Fig. 3.2) projected in the TCF ZX plane. In picking operations, the eyes follow the hand movements so the *neck twisting* is taken as the angle between the X-axis and the

projection of the vector from the head to the engaged hand wrist (10 or 6 in Fig. 3.2) into the TCF XY plane.

- The *trunk twisting* angle is computed as the angle between the GCF Y-axis and the projection of the vector from the left (4 in Fig. 3.2) to the right (8 in Fig. 3.2) shoulder into the GCF XY plane. While the *side bending* angle is the one between the GCF Z-axis and the vector from the spine base (0 in Fig. 3.2) and the shoulder spine (20 in Fig. 3.2) projected into the GCF ZY plane. The *trunk flexion/extension* degree is trivially assessed as the angle between the Z-axis and the projection of the vector from the spine base to the shoulder spine into the GCF ZX plane.

- The *right leg flexion* is assessed computing the angle between the vector from the right knee (17 in Fig. 3.2) to the right hip (16 in Fig. 3.2) and the vector from the right knee to the right ankle (18 in Fig. 3.2). Similarly for the *left leg flexion*.

- The *right upper arm flexion/extension* is computed as the angle between the RSCF Z-axis and the vector from the right shoulder (8 in Fig. 3.2) to the right elbow (9 in Fig. 3.2). Similarly for the *left upper arm flexion/extension*. As reported in [15], the quantitation of shoulder movement is difficult, because composed flexion/extension and abduction movement can take place at the same time, so that at least two coordinates are needed. Therefore, the *right* and *left arm abduction* angles are divided into two angles. For the right arm, the first angle, denoted as the *front abduction angle*, is the one between TCF Z-axis and the projection of the vector from the right shoulder to the right elbow into the TCF ZY plane. The second angle, *top abduction angle*, is the one between the RSCF X-axis and the vector from the right shoulder to the right elbow projected into the RSCF YX axis. The angles are computed in a similar way for the *left arm abduction*. The *right shoulder raising* is computed as the angle

between the vector from the shoulder spine and the right shoulder, in a relaxed standing position, and the same vector in the working position, both of them projected into the TCF ZY plane.

- The *Right lower arm flexion* is assessed computing the angle between the vector from the right elbow (9 in Fig. 3.2) to the right shoulder (8 in Fig. 3.2) and the vector from the right elbow to the right wrist (10 in Fig. 3.2). Similarly for the *left lower arm flexion*.
- The *right wrist flexion/extension* angle is computed as the one between the RWCF X-axis and the projection of the vector form the right wrist (10 in Fig. 3.2) and the right-hand tip (23 in Fig. 3.2) on the RWCF ZX plane. Similarly for the *left wrist flexion/extension*. The *right wrist midline bending* is computed as the angle between the RWCF X-axes and the vector from the right wrist to the right-hand tip projected on the RWCF YX plane.

To compute a score based on joint angles, the REBA method involves applying joint angle thresholds. These thresholds have been accurately defined for some joint axes in the REBA standard [13], but they have not been defined for others, such as upper arm abduction/adduction. For this body movement, the threshold is found experimentally recording the corresponding movement (e.g. repeated trunk twisting) and computing the associated angle at which it takes place. These thresholds are reported in Tab. 3.1. Moreover, some body movements, such as neck side bending and wrist-twisting, were not recorded due to a lack of Kinect accuracy so, these body positions are not considered in the computing of the REBA score.

3.2.3 Experimental procedure

In this section, the experimental setup and procedure used to identify $A'(\underline{\vartheta})$ and $B(\underline{\varphi})$ for different height position of the objects and different height of operator is briefly presented, from which the identified ergonomic function $\hat{C}$ will be derived in the next section.

Body Movement	Degrees
neck twisting	10
trunk side bending	10
trunk twisting	3.8
front abduction	10
top abduction	15
radial deviation	10.1
ulnar flexion	-5.1

Table 3.1: Experimental angle thresholds.

The experiment involved three volunteers of the height of 187, 180 and 167 cm respectively, two right-handed and one left-handed. The joints data collection was carried out as follows: the subject was asked to reach the maximum achievable object height on a wire marked every 7 cm, that indicates the object height, and then move to the object levels below, recording each time the body joint positions $\underline{\vartheta}$, $\underline{\varphi}$ in the task of picking the object. Each volunteer's experiment ended when the occlusion due to overlapping segments of the body became excessive, leading to the sole inference of the lower body joints, and so to the unreliability of the body joint positions.

One of the main problems when assessing work tasks with the Kinect is the occurrence of occlusions mainly due to object manipulation and overlapping of body segments. To minimize this side effect the Kinect was placed in an elevated position so that the arm-trunk overlap was reduced, and instead of using physical objects was used the marked wire that tells to volunteer at which height is the object to be taken. The results of this experiment are reported and discussed in the next section. Figure 3.4 shows the experimental setup.

Figure 3.4: Experimental setup used to identify A' and B.

3.3 Results

Fig. 3.5 reports the computed REBA score C_0, i.e. with zero weight objects, with the angles returned by the experiment.

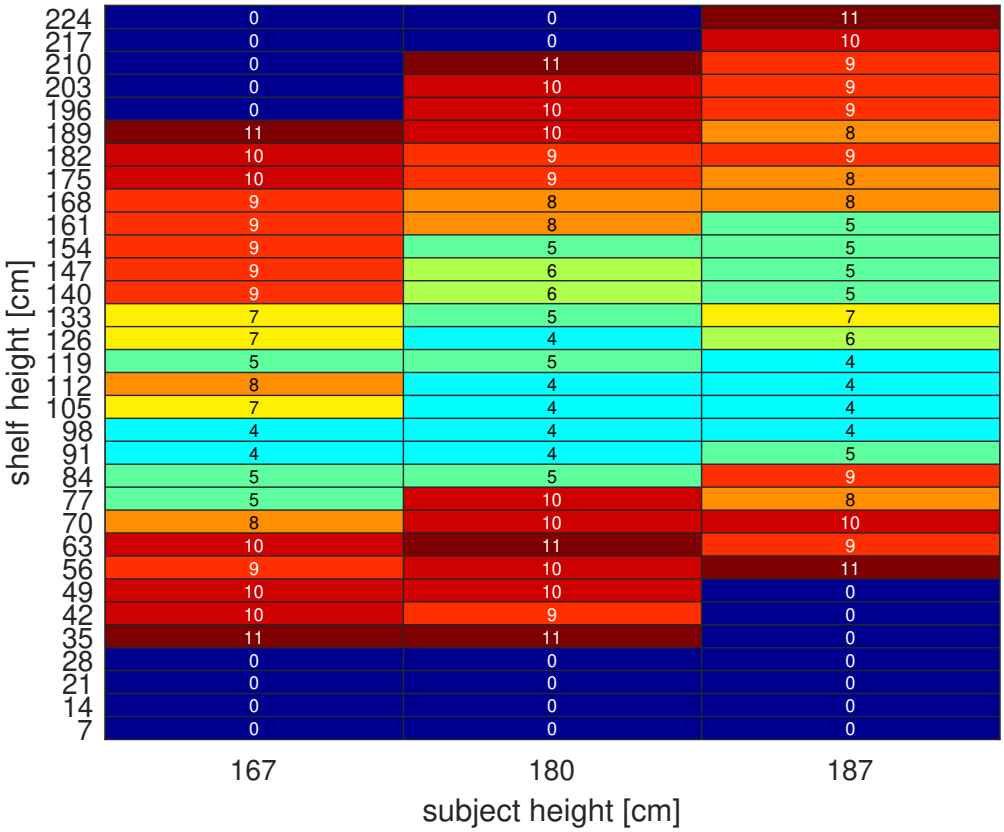

Figure 3.5: Experimental results for the REBA score C_0 for different object height and subjects.

These results show that, as expected, there are three main areas: an upper zone where the effort is elevated due to a high degree of flexion of the upper arm and wrist combined with a near full extension of the lower arm. A central comfort zone and, finally, another high-effort area mainly due to a combination of the trunk, legs, and arm flexion and extension of the lower arm. The top zero REBA zone is the unreachable area for the volunteers, while the one below is due to the interruption of the experiment due to too much body occlusion.

Starting from these $A'(h_w, h_o)$ and $B(h_w, h_o)$, obtained computing the REBA angles from the data returned by the Kinect tracking algorithm, for three different worker heights and different object height position, the ergonomic function

$$\hat{C} = \hat{C}(h_w, h_o, w) \tag{3.3}$$

is identified. Instead of taking as input the body joint angles and weight of the object to be taken as (3.1), it takes as input the height of the human worker and the weight and height position of the object and associates a REBA score to its picking action. For the missing data on the bottom, $\hat{C}$ assigns a weight based on the last A' and B data available. In Fig. 3.6 a comparison between experimental C' scores and the ones returned by $\hat{C}$ with zero weight objects is reported. As can be seen the estimated REBA scores are quite similar to the experimental ones.

Fig. 3.7 shows an example of $\hat{C}$ with zero object weight and $\hat{C}$ with random object weights, reported in the central column. As it can be seen that same weights in different height positions, such as those at 133 cm, 105 cm and 56 cm, do not have the same influence on the REBA score, in the first two cases, it increases by two points while in the latter one by only one point, or that the introduction of a heavyweight may not result in a REBA score change as in the case of an object at 63 cm.

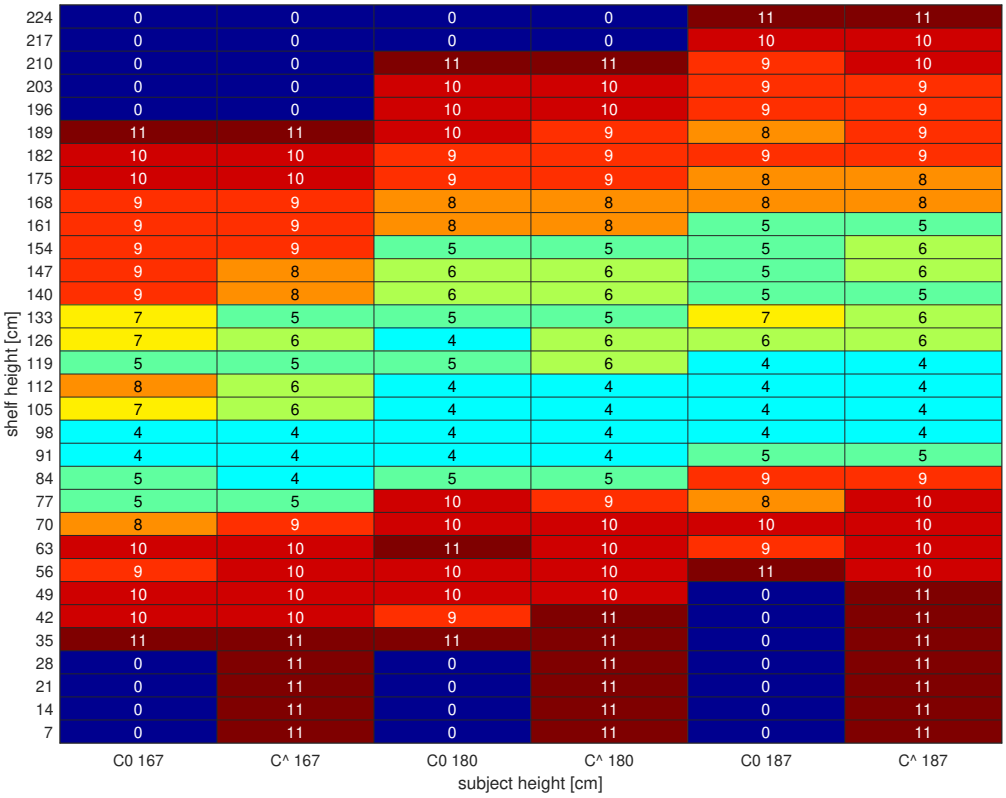

Figure 3.6: Comparison between experimental partial REBA scores C_0 and ergonomic function E one for different object height positions and worker heights.

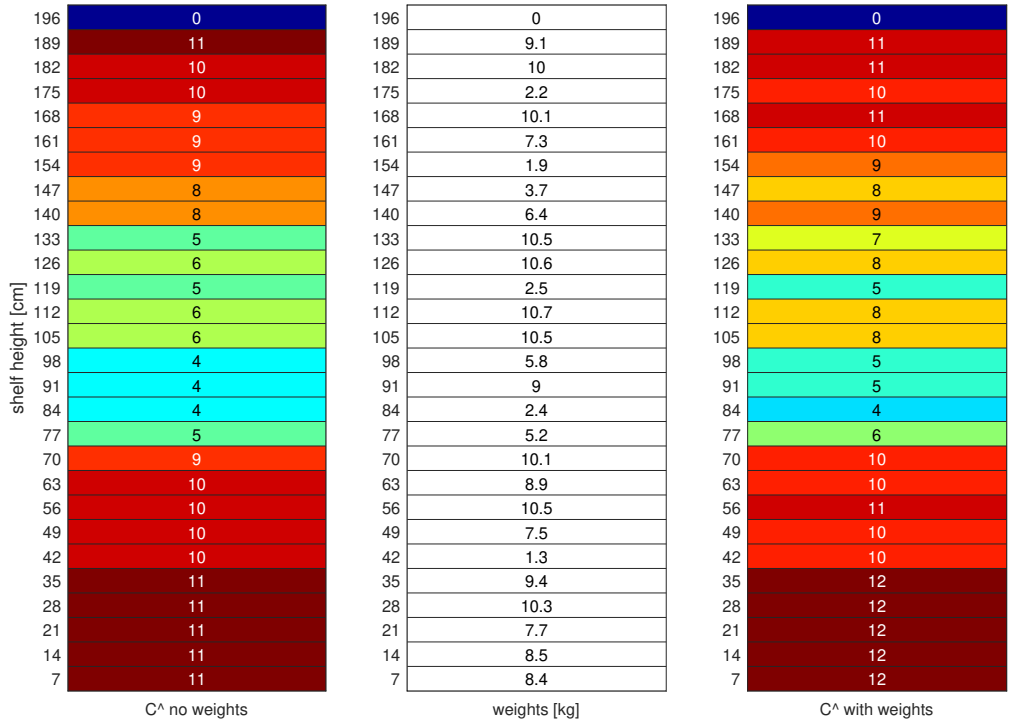

Figure 3.7: Comparison between $\hat{C}$ without object weights and $\hat{C}$ with random object weight for different object height position.

Chapter 4

Scheduling Algorithm

As already discussed in the Introduction, the aim of this work is to achieve human-robot kitting collaboration in a shared environment optimizing makespan and ergonomics of the process. This is done through a scheduling algorithm that allocates work between a single human and a single robot.

The next section presents the algorithm that realizes the human-robot coordination assigning objects to both of them.

4.1 Scheduler

In this thesis, the allocation and scheduling of objects to be taken between a human and a robotic worker is considered as a multiagent coordination problem with temporal and spatial constraints formulated as a mixed-integer linear programming (MILP) as in [11] and [20]. MILP is a mathematical optimization or feasibility program in which only some of the variables are constrained to be integers, while other variables are allowed to be non-integers. Although this approach does not scale well into large-scale problems due to its exponential computational complexity, the minimal team composition, involving a single human and a single robot, and the relatively small kit size considered, in term of number of objects, allowed

its efficient use and the capability for on-the-fly replanning in response to schedule disturbances. Online rescheduling is an important scheduler feature when a collaboration between robots and humans is carried out because it's necessary to be able to re-adjust the process schedule time due to the completion time variability of a human task.

The goal of the MILP scheduler is to allocate objects to individual workers and determine the sequence of picking actions such that time, human physical stress, or both factors are minimized. The MILP input consists of the information on the kit to be made and information about the current status of the process. The scheduler enforces a set of constraints representing time sequence, spatial restriction, capabilities of the robotic worker and basic job assignment rules. The output of the MILP is a set of objects assigned to the human and to the robot, the order and the time at which the objects are taken. Before going into details of the mathematical formulation of the MILP, in the following, the kitting workstation and all parameters and variables are presented.

4.2 Kitting workplace

To develop the scheduling algorithm, we consider a kitting workplace where the human is positioned on the left side of the rack while the robot on the right one. The goal of the scheduler is to allocate the objects among the agents while avoiding their cross in picking action, enforcing a sort of moving separating line that changes in position during the kitting process. Fig. 4.1 shows the environment considered in this work and where the reference frame is placed (RF, represented in red in Fig. 4.1) for the spatial parameters defined in the following.

The input *spatial parameters* to the MILP are:

(a) The longitudinal position X_i of the object i with respect to the RF

(b) The longitudinal position of the human when a rescheduling takes place X^h_{ris} with respect to the RF

(c) The longitudinal position of the robot flange when the rescheduling takes place X^r_{ris} with respect to the RF

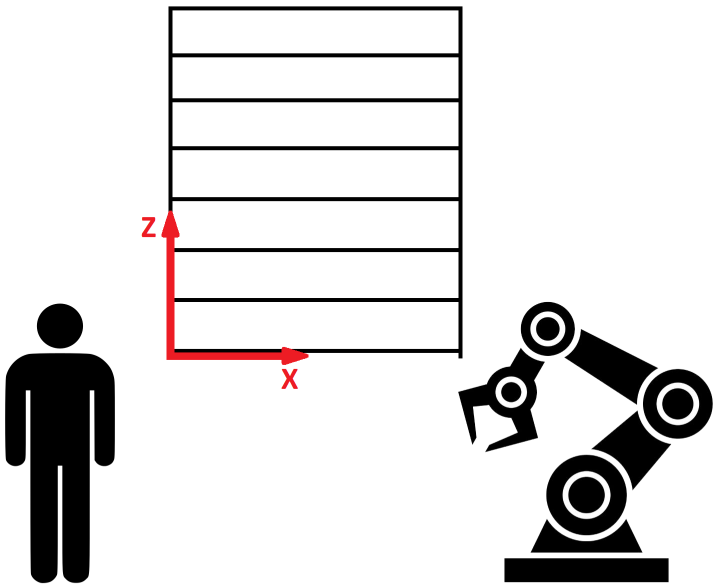

Figure 4.1: Workstation design considered in this work where the frame depicted in red is the reference one for the input spatial parameters of the MILP.

4.3 MILP model

Besides the spatial parameters, input to the MILP includes a set of objects to be picked $\mathbf{K} = \{i\}$, parameters related to the objects, the process status and additional parameters as outlined in the following. It takes as input also some sets used to enforce spatial and temporal constraints.

- *Object parameters:*

(a) The expected duration D_i^h and D_i^r required to complete the picking action of the object i for human and robot, respectively.

(b) The human strain s_i to pick the object i, as given by the identified ergonomic function in equation (3.3).

(c) *Capability Indicators Defined at the Object Level*: Capability information about the robot is provided to the optimizer as a binary parameter $B_i \in \{0, 1\}$, where $B_i = 1$ implies that the robot can pick the object i. For example, robotic workers cannot reasonably perform certain picking actions due to reachability limitations. Furthermore, the robot may not have appropriate end-effectors to perform the picking of some specific objects. Given that the focus of this thesis si to integration collaborative robots into the existing manual kitting process, the human worker is considered capable of performing all picking actions. However, in case a specific kitting process includes objects that human workers cannot pick, capability indicators for both human and robot workers can be defined.

- *Process status parameters:*

(a) A binary parameter $F \in \{0, 1\}$. $F = 1$ means that we are in a first scheduling state, otherwise we are in a rescheduling one.

(b) *Remaining time when rescheduling takes place*: In the formulation of the kitting process, it's assumed that the single picking action of both agents cannot be stopped when it started. Since the reschedule can take place at any time in the kitting process of the kit $\mathbf{K}$, the scheduler algorithm must account for the remaining time of picking action performed at the moment of the rescheduling by both human worker and robot. These values are reported as T_{rem}^h for the human and as T_{rem}^r for the robot.

(c) The upper bound on cycle time T_{max} greedily approximated by summing the longest picking duration for each objects o_i and

the longest remaining time among the two agents

$$T_{max} = \sum_{i \in \mathbf{K}} \max(D_i^h, D_i^r) + \max(T_{rem}^h, T_{rem}^r)$$

(d) The upper bound on the physical strain S_{max} that is equal to the total physical strain value for the scenario where all objects are taken by the human worker

$$S_{max} = \sum_{i \in \mathbf{K}} s_i$$

- *Additional parameters:*

  (a) The expected duration T_b needed to change the completed kit box with an empty new one at the end of the kitting task.

  (b) M, a large positive number used to encode conditional constraints

  (c) A weight parameter $\alpha \in \{ 0, 1 \}$ that represents the importance of minimizing makespan over strain.

- *Sets*:

  (a) The set L of object i such that the object i can be picked by the robot and its picking duration is less than the change box time:

  $$L = \{ i \in \mathbf{K} \mid D_i^r < T_b \wedge B_i \}$$

  (b) The set R of object pair (i, j) such that the object i can be picked by the robot and its longitudinal coordinate on the rack X_i is less than or equal to the object j one X_j:

  $$R = \{ (i, j) \mid i, j \in \mathbf{K} \wedge B_i \wedge X_i \leq X_j \wedge i \neq j \}$$

  (c) The set I^h of objects i such that the longitudinal position of the object i, is greater than or equal to the rescheduling robot

position X^r_{ris} and the human remaining time is less than or equal to the robot remaining time :

$$I^h = \{\, i \in \mathbf{K} \mid X_i \geq X^r_{ris} \wedge T^h_{rem} \leq T^r_{rem} \,\}$$

(d) The set I^r of objects i such that it can be picked by the robot, the longitudinal position of object i is less than or equal to the rescheduling human position X^h_{ris} and the robot remaining time is less than or equal to the human remaining time:

$$I^r = \{\, i \in \mathbf{K} \mid B_i \wedge X_i \leq X^h_{ris} \wedge T^r_{rem} \leq T^h_{rem} \,\}$$

The sets R, I^h and I^r are based on the workstation design considered in Fig. 4.1. Therefore, if the agents' positions with respect to the rack are changed (i.e human worker on the right and robot on the left), the spatial inequality sign has to be changed.

Based on the inputs values and a set of constraints, the optimizer attempts to solve for the variables listed as follow:

(a) binary decision variables $H_i \in \{0, 1\}\ \forall i \in \mathbf{K}$ indicating the assignment of the object i to the human worker if $H_i = 1$ or to the robot if $H_i = 0$.

(b) binary decision variables $J_{ij} \in \{0, 1\}\ \forall i, j \neq i \in \mathbf{K}$ specifying the relative sequencing of two objects i and j. $J_{ij} = 1$ implies that picking of object i occurs before object j.

(c) positive variables $t_i\ \forall i \in \mathbf{K}$ representing the picking starting time of the object i.

(d) $T_{\mathbf{K}}$, a positive variable representing the makespan, i.e. the completion time of the kit $\mathbf{K}$.

(e) $\Gamma_{\mathbf{K}}$, a positive variable representing the physical strain based on the scheduler output.

(f) two binary auxiliary variables n, m used to enforce the continuity of the human worker picking actions

All parameter inputs, sets, and variables used by the optimizer are summarized in Tab. 4.1.

The mathematical formulation of the problem is first presented through logical formulation to better understand how constraints work. Then, a linear form of constraints is described. The cost function f is formulated as a trade-off between the makespan and the total strain perceived by the human worker as in [20].

$$\min f = \alpha \cdot \frac{T_{\mathbf{K}}}{T_{max}} + (1 - \alpha) \cdot \frac{\Gamma_{\mathbf{K}}}{S_{max}}$$

subject to

1) Objects i should be assigned to the robots only if it's capable of picking the object

$$H_i = 1 \quad \forall i \in \mathbf{K} : \neg B_i$$

2) Human and robot should not cross their picking action during the kitting process. So, if the object i is assigned to the robot the associated picking operation must start and finish before or after the object j if this object is assigned to the human worker.

$$\neg H_i \wedge H_j \wedge J_{ij} \implies t_j \geq t_i + D_i^r \quad \forall i, j \in R$$

$$\neg H_i \wedge H_j \wedge \neg J_{ij} \implies t_i \geq t_j + D_j^h \quad \forall i, j \in R$$

This allows ensuring a safety spatial separation between the two agents during the kitting process.

3) Human worker and robot only perform one picking action at a time, if two objects i and j are assigned to the same agent the object i must start and end before or after the object j

$$H_i \wedge H_j \wedge J_{ij} \implies t_j \geq t_i + D_i^h \quad \forall i, j \neq i \in \mathbf{K}$$

Parameters	Description
X_i	Longitudinal position of the object i
X^h_{ris}	Human longitudinal position when rescheduling takes place
X^r_{ris}	Robot flange longitudinal position when rescheduling takes place
D^h_i	Estimated human picking duration for the object i
D^r_i	Estimated robot picking duration for the object i
s_i	Physical effort for pick object i
B_i	Binary indicator if the robot can pick the object i
F	Binary indicator if the algorithm performs a rescheduling
T^h_{rem}	Human picking action remaining time
T^r_{rem}	Robot picking action remaining time
T_{max}	Upper bound on cycle time
S_{max}	Upper bound on physical effort
Tb	Estimated change box duration
M	Positive number used to enforce conditional constraints
α	weighted importance of time over ergonomics
Sets	**Description**
R	Set of (i, j) object pairs such that $X_i \leq X_j$
L	Set of objects i such that $D^r_i < T_b \wedge B_i$
I^h	Set of objects i such that $X_i \geq X^r_{ris} \wedge T^h_{rem} \leq T^r_{rem}$
I^r	Set of objects i such that $B_i \wedge X_i \leq X^h_{ris} \wedge T^r_{rem} \leq T^h_{rem}$
Variables	**Description**
H_i	Boolean indicating object i is assigned to human or robot
J_{ij}	Binary sequencing variable of two objects i and j
t_i	Picking starting time of object i
$T_{\mathbf{K}}$	Resulting cycle time based on scheduler output
$\Gamma_{\mathbf{K}}$	Total physical effort based on scheduler output
n, m	Auxiliary variables

Table 4.1: Scheduler parameters, sets, and variables.

$$H_i \wedge H_j \wedge \neg J_{ij} \implies t_i \geq t_j + D_j^h \quad \forall i, j \neq i \in \mathbf{K}$$

$$\neg H_i \wedge \neg H_j \wedge J_{ij} \implies t_j \geq t_i + D_i^r \quad \forall i, j \neq i \in \mathbf{K} : B_i \wedge B_j$$

$$\neg H_i \wedge \neg H_j \wedge \neg J_{ij} \implies t_i \geq t_j + D_j^r \quad \forall i, j \neq i \in \mathbf{K} : B_i \wedge B_j$$

4) When the scheduler makes the first scheduling of the kit ($F = 1$), the human first changes the completed box with an empty one, before starting the next picking actions, while the robot can start to pick the objects with an associated picking duration longer than the human worker change box duration

$$H_i \implies t_i \geq T_b \quad \forall i \in \mathbf{K}$$

$$\neg H_i \implies t_i \geq T_b \quad \forall i \in L$$

5) When the scheduler makes a rescheduling ($F = 0$), the objects placed in the area occupied by an agent, if assigned to the other one, must start after that the first agent had ended its picking action

$$H_i \implies t_i \geq T_{rem}^r \quad \forall i \in I^h$$

$$\neg H_i \implies t_i \geq T_{rem}^h \quad \forall i \in I^r$$

6) When the scheduler makes a rescheduling ($F = 0$), the agents start the next picking action after their remaining time

$$H_i \implies t_i \geq T_{rem}^h \quad \forall i \in \mathbf{K} : i \notin I^h$$

$$\neg H_i \implies t_i \geq T_{rem}^r \quad \forall i \in \mathbf{K} : i \notin I^r$$

7) As reported in [4], in the picking process it is desirable that the material picker can pick directly the next object without waiting for another material picker, to give continuity to picking activities and reduce time losses. It's then introduced a constraint that enforces continuity in human picking actions. Each time a rescheduling takes place, if an object i is assigned to the human worker, it's picking

action must end in the interval from T_b or T^r_{rem} or T^h_{rem}, depending on F and y, and the sum of the picking duration of all the objects assigned to the human

$$H_i \implies t_i + D^h_i \leq \sum_{j \in \mathbf{K}} H_j D^h_j + T_b\ F + (T^h_{rem}\ m + T^r_{rem}\ n) \neg F \quad \forall i \in \mathbf{K}$$

$$n = H_i \vee \cdots \vee H_j \quad \forall i, j \neq i \in I^h$$

$$m = Hi \vee \cdots \vee H_j \quad \forall i, j \neq i \in \mathbf{K} : i, j \notin I^h$$

These last two variables are used to asses if the human starts its first picking action after the human picking time $m = 1$ or after the robot picking time $n = 1$.

8) The kit is completed when all its objects have been taken

$$t_i + D^h_i H_i + D^r_i \neg Hi \leq T_{\mathbf{K}} \leq T_{max} \quad \forall i \in \mathbf{K}$$

9) The total physical strain is equal to the sum of the object physical effort score assigned to the human worker

$$\sum_{i \in \mathbf{K}} H_i\ s_i = \Gamma_{\mathbf{K}}$$

The linear mathematical formulation, computed using the method illustrated in [3], is presented below:

$$\min f = \alpha \cdot \frac{T_{\mathbf{K}}}{T_{max}} + (1 - \alpha) \cdot \frac{\Gamma_{\mathbf{K}}}{S_{max}}$$

subject to:

$$
\begin{aligned}
H_i &= 1 && \forall i : \neg B_i \\
t_i - t_j - MH_i + MH_j + MJ_{ij} &\leq 2M - D_i^r && \forall i, j \in R \\
-t_i + t_j - MH_i + MH_j - MJ_{ij} &\leq M - D_j^h && \forall i, j \in R \\
-t_j + t_i + MH_i + MH_j + MJ_{ij} &\leq 3M - D_i^h && \forall i, j \neq i \in \mathbf{K} \\
t_j - t_i + MH_i + MH_j - MJ_{ij} &\leq 2M - D_j^h && \forall i, j \neq i \in \mathbf{K} \\
-t_j + t_i - MH_i - MH_j + MJ_{ij} &\leq M - D_i^r && \forall i, j \neq i : B_i \wedge B_j \\
t_j - t_i - MH_i - MH_j - MJ_{ij} &\leq -D_j^r && \forall i, j \neq i : B_i \wedge B_j \\
-t_i + MH_i &\leq M - T_b && \forall i \in \mathbf{K} \\
-ti - MH_i &\leq -Tb && \forall i \in L \\
-t_i + MH_i &\leq M - T_{rem}^r && \forall i \in I^h \\
-t_i - MH_i &\leq M - T_{rem}^h && \forall i \in I^r \\
-t_i + MH_i &\leq M - T_{rem}^h && \forall i \in \mathbf{K} : i \notin I^h \\
-t_i - MH_i &\leq M - T_{rem}^r && \forall i \in \mathbf{K} : i \notin I^r \\
-\sum_{j \neq i \in \mathbf{K}} H_j D_j^h \; + t_i \; + (M - D_i^h)H_i + & \\
(T_{rem}^r \, n - T_{rem}^h \, m)(1 - F) &\leq M - D_i^h + T_b F && \forall i \in \mathbf{K} \\
H_i - n &\leq 0 && \forall i \in I^h \\
H_i - m &\leq 0 && \forall i \in \mathbf{K} : i \notin I^h \\
n - \sum_{i \in I^h} H_i &\leq 0 && \\
m - \sum_{i \in \mathbf{K} : i \notin I^h} H_i &\leq 0 && \\
t_i + D_i^h H_i - D_i^r H_i - \Gamma_{\mathbf{K}} &\leq D_i^r && \forall i \in \mathbf{K} \\
T_{\mathbf{K}} &\leq T_{max} && \\
\sum_{i \in \mathbf{K}} s_i H_i - \Gamma_{\mathbf{K}} &= 0 &&
\end{aligned}
$$

4.4 Kit schedule flow

In the following, the behavior of the scheduling algorithm for a set of kits **P** is described, highlighting when the reschedule takes place during the preparation of a single kit **K**. At the beginning the algorithm receives the information about the first kit to be made. Then, the *status parameter* F is set to one, the MILP is solved which returns a schedule where some objects are assigned to the human worker and others to the robot and the agents start their tasks. During the kitting preparation, the reschedule takes place when one of these events occur:

- the human worker finishes his picking action or the box change;
- the robot should start his next picking action but this will cause a cross between the human and the robot. Theoretically, this is avoided by the MILP optimization, however during the execution of the kitting process, the human may take more time to pick the scheduled object, so the current schedule is no more valid.

Each time that a reschedule takes place, the MILP considers the problem as a new kit, i.e the MILP algorithm receives as input only the set of unpicked objects, the *status parameter* F is set to zero and the input *spatial and temporal sets* are built according to the new *spatial parameters* and *status parameters*. Then the old schedule is updated with the new one.

Figure 4.2 highlights the algorithm as a flow diagram, where **H** and **R** stand for the human worker and robot, respectively. Fig. 4.3 shows a schedule example returned by the MILP optimization, where over each picking action the object picked is reported and in the middle, the object position in the rack is shown. As can be seen, the robot can start its picking action while the human is changing the box (one to eleven seconds) and human and robot does not cross their picking action during the kit preparation.

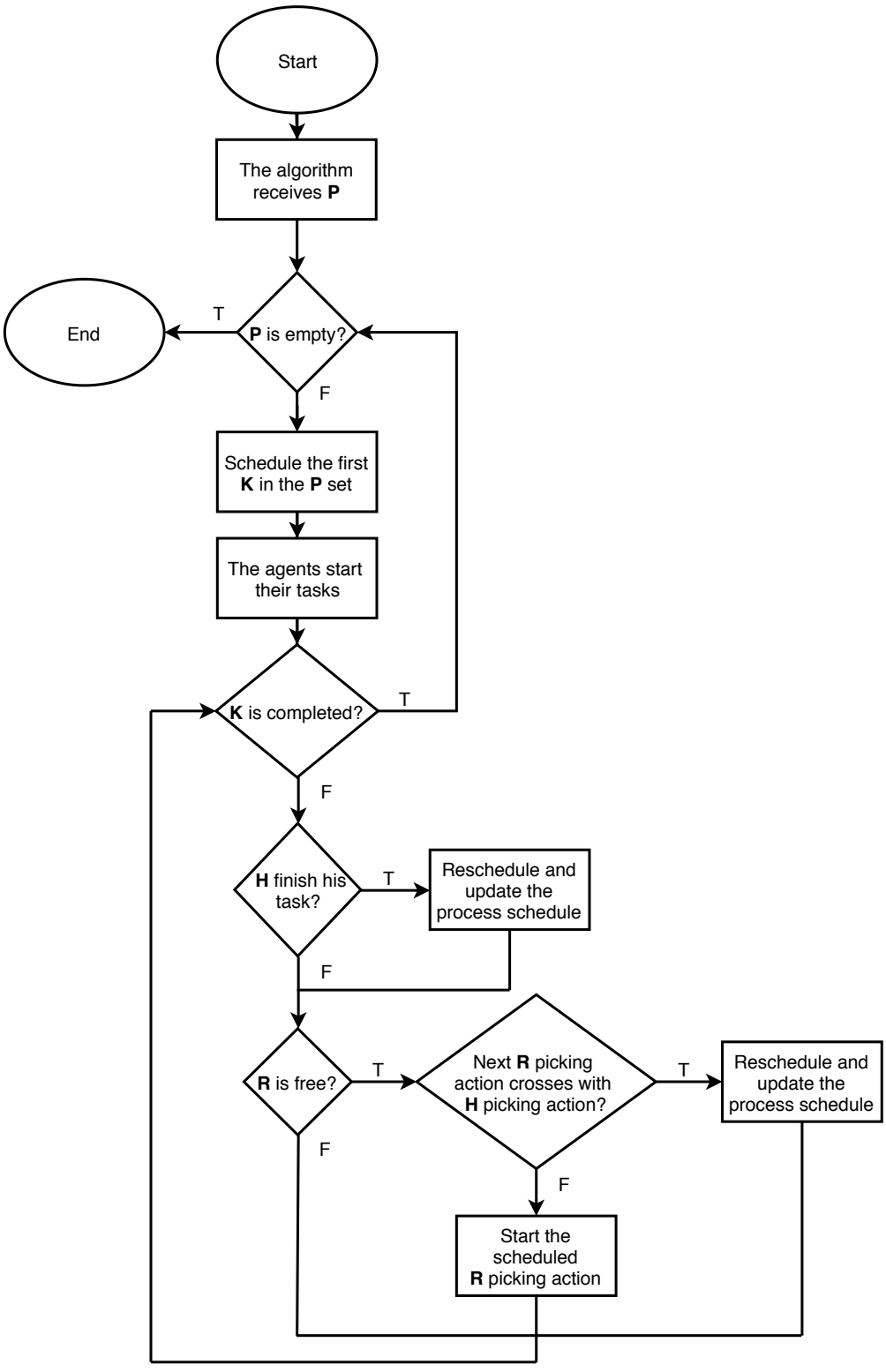

Figure 4.2: Scheduling algorithm flow where: **P** is the set of kits to be made,**K** is the single kit belonging to **P**, **H** is the human worker agent while **R** is the robot one.

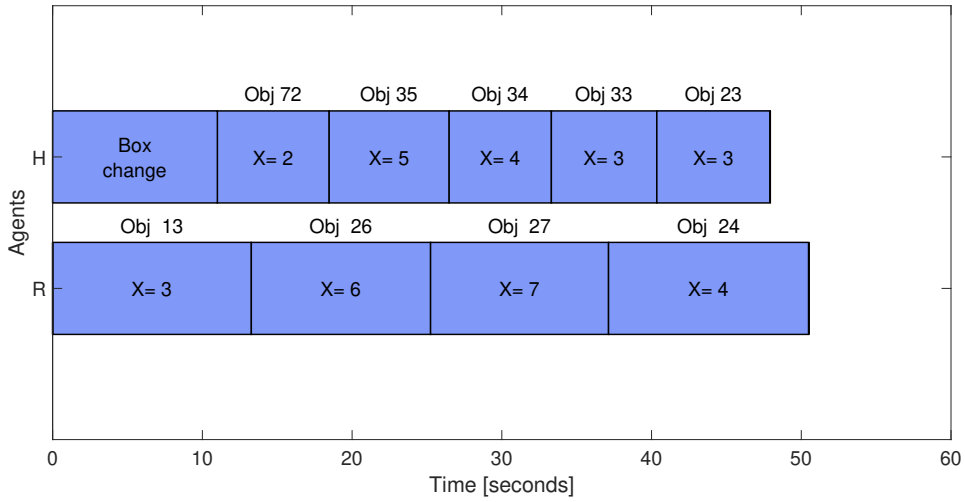

Figure 4.3: Gantt chart of a scheduled kit. Over each picking action duration the number of the object picked is reported while in the center the object rack position is reported.

Chapter 5

Experimental Results

This chapter presents the results obtained by applying the developed scheduling algorithm to the human-robot kitting system. Firstly, the experimental set-up is described in Section 5.1. Secondly, Section 5.2 presents the results of the scheduling algorithm, performed through simulations. Finally, the outcome of real experiments is described in Section 5.3.

5.1 Experimental set-up

The scheduling algorithm developed in this thesis has been tested on an experimental set-up that aims at simulating a realistic kitting system. In Fig. 5.1 it is possible to see all the equipment needed for the experiments:

- a robotic system, which is composed of an industrial manipulator endowed with a vacuum gripper and its control unit;
- a gravity rack with different size boxes that represent the objects to be taken to complete the kit
- a screen connected to the external computer used to tell the human worker which object has to be taken
- a button used to communicate through the robot to the external

computer that the human worker has finished his picking action or the box change

Figure 5.1: Kitting system simulation.

5.1.1 Robotic system

The robot used in this project is a *Comau Smart SiX* industrial manipulator (see Fig. 5.2a), produced by Comau [5], which is a 6 degree-of-freedom serial robot with a maximum payload of 6 kg and a maximum horizontal reach of 1400 mm.

The robot is equipped with a C4G control unit, that provides all functions for motion control. In the following a brief description of the main features of the robotic manipulator are presented. Among all information that are present on the Comau Smart Six datasheets, it is of fundamental importance to know the limits of the robot joint rotations, which define the working region depicted in Figure 5.2b:

$$\begin{bmatrix} \mathbf{q}_{min} \\ \mathbf{q}_{max} \end{bmatrix} = \begin{bmatrix} -170° & -85° & -170° & -210° & -130° & -2700° \\ 170° & 155° & 0° & 210° & 130° & 2700° \end{bmatrix}$$

Also, limits to the maximum achievable joint velocity are present, which amount in absolute values to:

$$\dot{\mathbf{q}}_{max} = \begin{bmatrix} 140°/s & 160°/s & 170°/s & 450°/s & 375°/s & 550°/s \end{bmatrix}$$

However, for safety reasons reduced velocity bounds have been used during experiments.

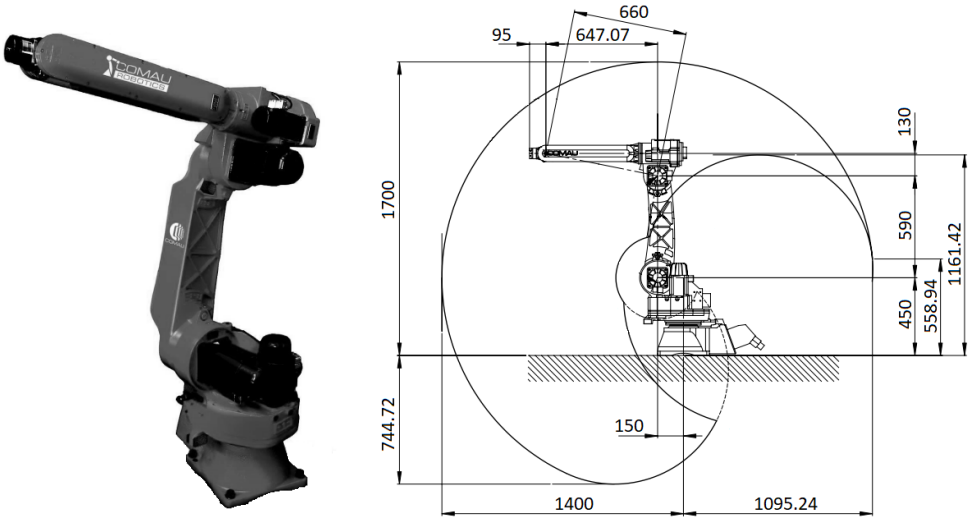

(a) Comau Smart Six. **(b)** Working range.

Figure 5.2: Image of the Comau Smart Six industrial manipulator and its working range.

The Comau C4G controller can operate in two different modes: standard mode and open mode.

The standard Comau C4G controller consists of modular architecture with three different hierarchical hardware levels. The first level is the System Master Processor (SMP+) control board. At this level, all high level processes take place: interpretation of user programs, management of operator interfaces, network communications, trajectory generation, computation of dynamic model and management of assigned tasks, collisions detection, system diagnostics, high hierarchical level centralized adjustment process, axes synchronizing control, management of all I/O devices. The

second level is the Model Predictive Control (MPC) board, inside: fine interpolation of the manipulator trajectory, robot position adjustment, real-time system diagnostics, master-slave axes management. The lower level is the Digital Signal Processing (DSP) board, inside: control of electric motor currents and torque generation process for individual axes control, power stage management, position sensor and acquisition of motor angular measurements, high speed digital and analogical I/O management. The system architecture is based on a real-time communication. It has a frame rate of 1ms on an Ethernet network that uses a UDP protocol, between the SMP+ board (client) and the MPC board (server). In a normal industrial environment, a human operator manages the robot behavior giving instructions to the control unit using the provided teach pendant or through a computer connected employing a LAN cable with the Comau software WinC4G.

The standard C4G controller allows us to include inputs from different kinds of sensors in the system path generation. On C4G architecture the robot trajectory interpolator receives, via PDL2 instructions, sensor signals and uses them to modify the planned trajectory according to the set of available parameters to tune the algorithm. A more flexible way to integrate sensor signal, in the Comau system, is the C4GOpen controller. The sensor signals are acquired by an external acquisition system, sent to the computer connected in real-time with the controller and used to modify the robot path planning. The PC adds power to the Robot Control Unit simplifying the implementation of complex manufacturing applications. In this way, writing custom applications where standard control processes and trajectory generation interact with external sensors, devices or PCs is feasible. Mixing trajectories between open and standard modalities is also possible, together with the possibility of programming the robot using different open modalities such as additional and absolute position control, additional current control, trajectory management and modification of pre-planned trajectory. The main difference between the two solutions,

in terms of data received by sensors, is the way the industrial controller receives them. The C4G Sensor Tracking option receives inputs from PDL2 programs; these signals are non-deterministic as the PDL2 interpreter is. The average time a path correction is applied, from sensor signal to robot, is about 20-30ms. On the other hand, the C4GOpen controller communicates via a real-time connection with a robot interpolator and can send the sensor corrections, every 1-2ms (see [22]).

Although Comau Smart Six is used for an industrial purpose and not for collaborative tasks, it was chosen because a large reachable area is required for this application. Also, since the robot is not endowed with external sensors and does not replan its trajectory but rather has to repeatedly perform the same operation, it has been chosen to use the standard controller connected through a TCP/IP connection to the external computer where the scheduling algorithm runs. Communication between the external computer and the C4G controller is explained in Section 5.1.3.

5.1.2 Gravity rack and objects

To simulate an industrial kitting system, a gravity rack was developed starting from two shoe racks with tilted shelves, on which different size guides have been created to hold boxes of three different dimensions representing the objects that need to be taken to form the kit, the size of the boxes are: 9 x 9 x 14 cm (length x width x height), 14 x 14 x 5 cm and 8 x 8 x 11 cm. In Fig. three different kinds of objects can be seen:

- boxes marked with a red cross means that the robot cannot pick it, some of which are actually out of the robot's reach while others are marked to simulate the robot's inability to manipulate them
- boxes with a label that shows a number between 5 and 6 that represents the object weight in kilograms
- boxes without a label and red cross that can be picked both by

human worker and robot, whose weight is below 5 kg and so it does not affect the ergonomic score of the object.

Figure 5.3a shows the rack with annotations of the dimensions. To enable the robot to pick the boxes, the industrial manipulator has been endowed with a vacuum gripper reported in Fig. 5.3b.

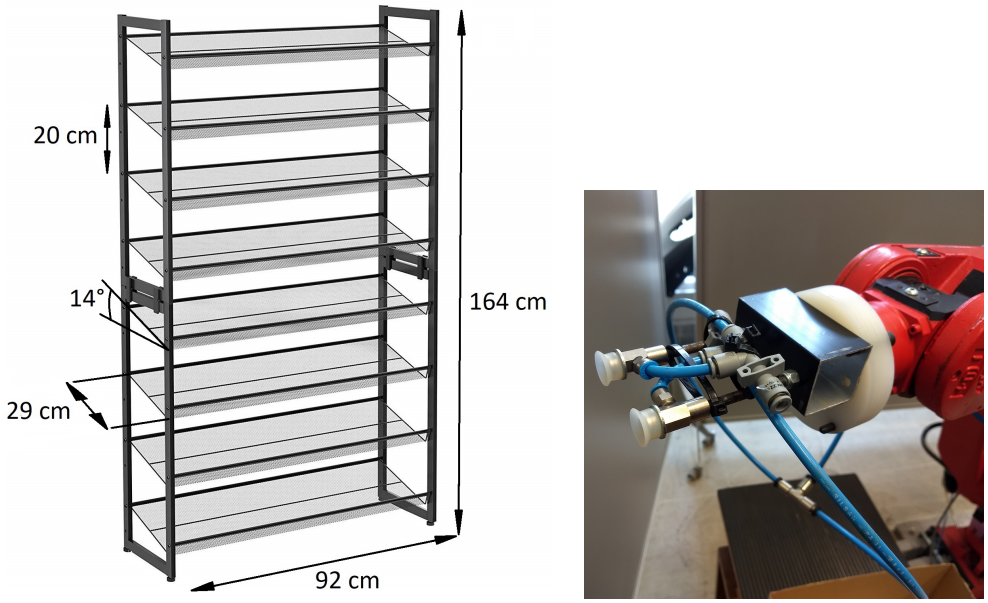

(a) Empty rack. **(b)** Vacuum gripper.

Figure 5.3: Image of the rack and the vacuum gripper used in the experimental set-up.

5.1.3 Interface between C4G and the external PC

For the scheduling algorithm to work online, some information must be communicated in real-time to the external computer by the C4G controller:

- the status of the robot, i.e. if the robot has completed its picking action or not, so that the scheduling algorithm can send the next task to the robot

- the longitudinal position of the robot flange X^r_{ris} that will be used as input to the MILP

- the status of human worker that is communicated through the button connected to the robot, that is the status of the button

To achieve this real-time communication, a software library has been developed based on a Server/Client architecture, in which the external computer and the controller communicate using TCP/IP sockets. More details about PDL2 sockets can be found in [28] where the author has written a library based on socket communication to program the Comau Smart Six in C++ instead of PDL2. For the client-side, which is the external computer, a library to deal with the transmission of the number of the object to be taken and receive the necessary information to the scheduling algorithm reported above. For the server-side, so the C4G controller, two programs have been implemented in PDL2 language [23]: the main program that deals with sending and receiving information from the external computer that manages the process, and another program that deals with the movement of the robot. The motion program contains all the trajectories to pick the robot reachable objects, then the robot performs a certain trajectory according to the command received by the main program which is in turn received from the external computer.

Figure 5.4 shows the architecture of the system, specifying the distinction between the client -ide and the server-side.

5.2 Simulation results

Before performing real experiments and evaluate the performance of the online scheduling algorithm in terms of makespan $T_{\mathbf{K}}$ and ergonomics $\Gamma_{\mathbf{K}}$, a study on how the tradeoff parameter α affects the output schedule was carried out through simulations and reported in the following.

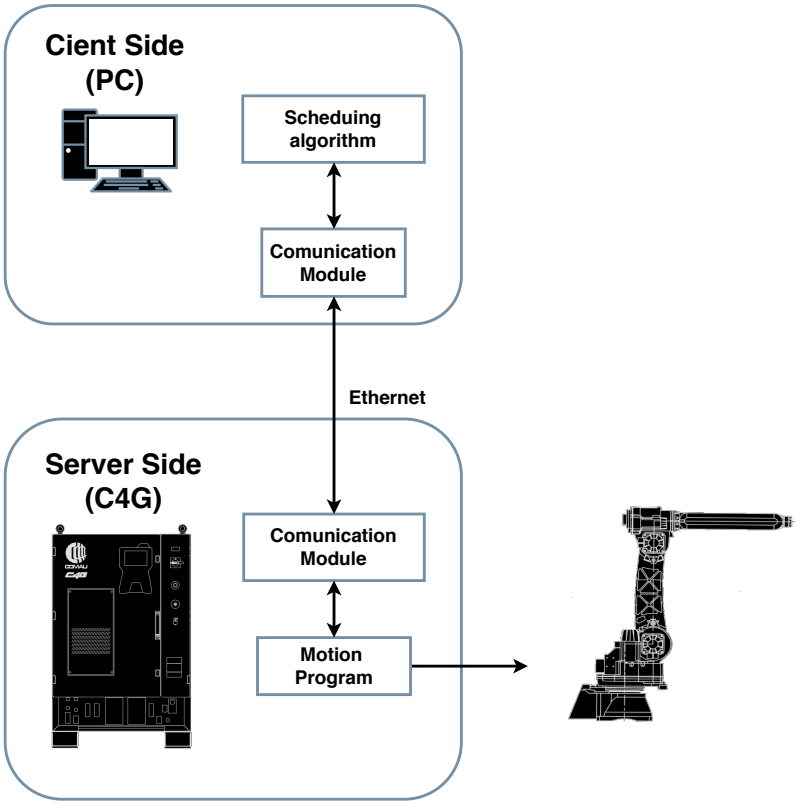

Figure 5.4: Communication between the software modules.

5.2.1 Makespan versus Total Strain

To better understand how α affects the schedule output, different size kit scheduling with random objects has been performed, varying α from 1 to 0.1 in decrements of 0.1. To retrieve the duration of the human picking action of an object i D_i^h the actual picking action was measured while the duration of the robot picking action D_i^r is determined by executing the robot trajectory to pick the object i and measure its time duration.

Figure 5.5 shows the tradeoff between makespan and total strain for three different kit sizes and values of α between 1 to 0.1. Blue dots are the makespan and total strain resulting from the human-robot collaboration varying alpha while the red dots are the baseline ones, i.e. the makespan and total strain when the human worker performs all the kits alone. Figure

5.6 shows the makespan (red line) and the total strain (blue line) average percentage improvement as α changes from 1 to 0.1. This makespan and total strain are obtained as the average of 100 simulated schedules.

From the results, it can be seen that makespan and total strain roughly vary inversely: as makespan increases, total strain decreases. In general, values at $\alpha = 0$ and $\alpha = 1$ tend to be skewed in one direction over the other, and values of α in the middle tend to show subtler tradeoffs. The makespan of a task may increase or decrease after introducing the collaborative robot depending on α, but the total strain cannot increase. We consider the strain of a picking action on the human worker to be 0 if the object is picked by the robot, and thus, any objects assigned to the robot will decrease the total strain. Therefore, we see noticeable improvements in total strain, as α approaches 0. Decreases in makespan compared with the baseline (red dots in fig 5.5) are less extreme since the Comau Smart Six speed and acceleration are highly reduced for safety reasons. Although the robot may take a longer duration to perform picking actions, having a second worker functioning in parallel with a human worker can still speed up the kit preparation as a whole. The behavior of the tradeoff remains quite the same varying the size of the kit so one can choose one value of α and keep the same along the kitting process. Fig. 5.6 helps to choose which aspect of the process improve the most:

- with $0.7 \leq \alpha \leq 1$ makespan and ergonomics have more or less the same average improvement
- with $0.4 \leq \alpha \leq 0.7$, there is a huge improvement in terms of physical strain almost without increase the makespan compared to the baseline one.
- with $\alpha \leq 0.4$ there is still an improvement in terms of ergonomics, however, the makespan starts to get worse compared to the baseline case

For values of α less than 0.3, there is a flattening of the two curves, this is

	Baseline	α									
		1	0.9	0.8	0.7	0.6	0.5	0.4	0.3	0.2	0.1
Makespan [s]	64.03	47.11	47.11	49	49	68.42	68.419	81.58	95.5	95.5	95.5
Total strain	45	31	31	27	27	13	13	8	4	4	4

Table 5.1: Baseline makespan and total strain and schedule output ones for different values of α for the same kit.

because there are objects which cannot be taken by the robot and therefore they must be picked by the human worker.

Figure 5.7 shows the schedules obtained for the same kit of eight objects with different values of α; the values of α omitted are the ones that produce the same schedule. As can be seen for $\alpha \leq 0.3$ there can be no further improvement because object number 31 cannot be reached by the robot. The baseline makespan and total strain together with the ones obtained by varying α are reported in Tab. 5.1.

5.3 Experiments

This Section presents the results obtained applying the designed scheduling algorithm to the kitting system described in Section 5.1. A first series of experiments have been conducted using the scheduling algorithm in an offline mode, i.e. during the kitting preparation there is no update of the schedule made at the beginning. Then another series of experiments have been conducted with the online scheduling algorithm presented in Section 4. The reason is that we wanted to see if an online scheduler could perform better than an offline one and absorb scheduling disturbances due to the variability of human worker picking times and evaluate the different performance.

In both scheduling approaches, three complete kitting cycles have been performed, which consist of several consecutive kits preparation. In each complete cycle, there were boxes to be prepared with a number of objects

between 6 and 9 randomly chosen, whose objects were also randomly chosen among those in the rack so that in a complete cycle at least 100 objects are picked. The value of α is kept fix to 0.8 which means that the scheduler tends to attain similar percentage improvements for both makespan and physical strain.

To give a better understanding of the execution of experiments, Figure 5.8 shows frames taken from a video of the human worker and robot performing a single kit. In Fig. 5.8a and 5.8b the robot starts its picking action while the human adds the objects picked by the robot of the previous kit to its box. Then, the human comes to his station with a new empty box and presses the button communicating to the computer that he had finished his task and can receive information about the next object to be picked (Fig. 5.8c). The scheduler notifies the human worker that the button has been pressed and shows to him through the screen which objects he should take (Fig. 5.8d). Then, the human worker and robot can work in parallel (see Fig. 5.8e and Fig. 5.8f) until the kit is completed. Finally, the operator can change the completed box with an empty one to start a new kit (see Fig. 5.8g) and a new kit cycle starts.

In the following, some performance indexes are defined and the experimental results obtained in the offline and online mode are presented.

- *The productivity of the i-th kit* $\boldsymbol{K}_i$:

$$\lambda_i = \frac{|\mathbf{K}_i|}{\overline{T}_{\mathbf{K}_i}}$$

  where $|\mathbf{K}_i|$ is the number of the objects contained in the i-th kit $\mathbf{K}_i$, and $\overline{T}_{\mathbf{K}_i}$ is the actual time required to complete the i-th kit $\mathbf{K}_i$.

- *The average strain of the i-th kit* $\boldsymbol{K}_i$:

$$e_i = \frac{\overline{\Gamma}_{\mathbf{K}_i}}{\sum_{j \in \mathbf{K}_i} \overline{H}_j}$$

where $\overline{\Gamma}_{\mathbf{K}_i}$ is the actual total strain upon the human worker at the end of the i-th kit $\mathbf{K}_i$ and the sum at the denominator is the number of objects collected by the human.

- *Productivity of a set of kits* $\boldsymbol{P}$:

$$\Lambda = \frac{\sum_{i=1}^{|\mathbf{P}|} \lambda_i \overline{T}_{\mathbf{K}_i}}{\sum_{i=1}^{|\mathbf{P}|} \overline{T}_{\mathbf{K}_i}}$$

that is the weighted average of the kits cycle productivity with respect to the duration of each kit.

- *The strain of a set of kits* $\boldsymbol{P}$:

$$E = \frac{\sum_{i=1}^{|\mathbf{P}|} e_i \overline{T}_{\mathbf{K}_i}}{\sum_{i=1}^{|\mathbf{P}|} \overline{T}_{\mathbf{K}_i}}$$

that is the weighted average of kits cycle average strain with respect to the duration of each kit.

- *Cost of the i-th kit* $\boldsymbol{K}_i$:

$$\overline{f}_i = \alpha \cdot \frac{\overline{T}_{\mathbf{K}_i}}{T^I_{max}} + (1-\alpha) \cdot \frac{\overline{\Gamma}_{\mathbf{K}_i}}{S^I_{max}}$$

where T^I_{max} and S^I_{max} are the upper bound on time and physical strain of the first schedule.

- *Cost of a set of kits* $\boldsymbol{P}$:

$$\Delta = \frac{\sum_{i=1}^{|P|} \overline{f}_i \, \overline{T}_{\mathbf{K}_i}}{\sum_{i=1}^{|\mathbf{P}|} \overline{T}_{\mathbf{K}_i}}$$

that is the weighted average of kits cycle resulting cost function with respect to the duration of each kit.

The results in terms of Productivity, Strain, and Cost of the two scheduling approach are reported in Figure 5.9. Figure 5.9a shows the weighted box plot of the cost function of a set of kits $\mathbf{P}$, where the red line represents the weighted median, the bottom blue line the weighted 25th percentile and the top one is the weighted 75th percentile, for the two scheduling approach. As it can be seen the online rescheduling approach is significantly better then the offline one with a decrease in the weighted median and the two percentiles of about 17%. This results in increased productivity and/or an increase in ergonomics. However, as can be seen in Fig. 5.9b and Fig. 5.9c the lower values of the cost Δ is mainly due to an increase of the productivity Λ, of 19% in the weighted median compared to the case without rescheduling, respect to a decrease of the Strain E which is anyway generally lower than the baseline case, with a decrease in the weighted median of 10%. The fact that productivity Λ increases much more than strain E decreases can be explained by noting that the scheduler online eventually ends up assigning an object that would originally be assigned to the robot, to the human worker that could increase the strain compared with the scheduler offline since generally the objects assigned to the robot are the ones with a higher physical effort score. Figure 5.10 shows an example of how the schedule evolves during the kitting process with the online algorithm.

Overall, the online scheduling algorithm proposed in this thesis enables human-robot kitting collaboration with good performance in terms of productivity and physical strain reduction compared to the one of an offline scheduler and moreover compared with the traditional human kitting process.

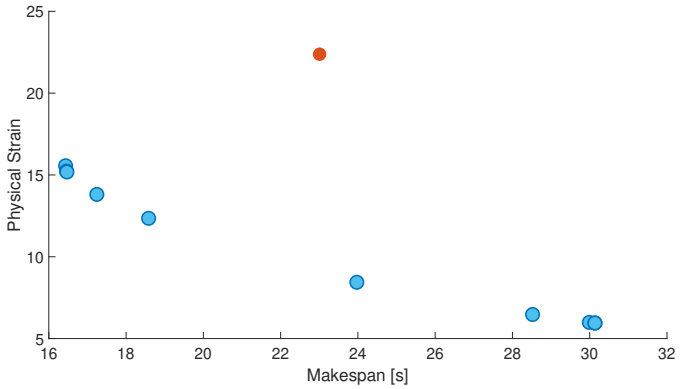

(a) Makespan and Total Strain results for a 3-objects kit.

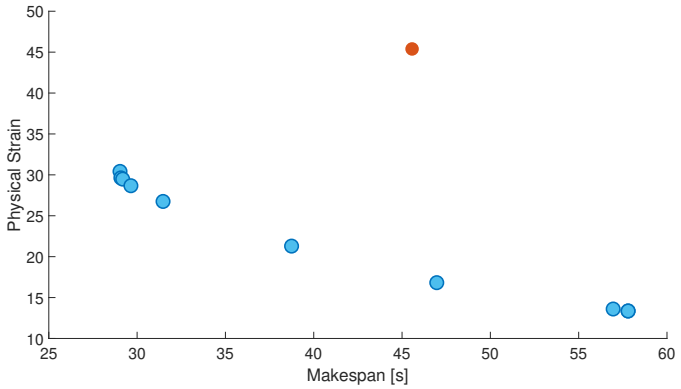

(b) Makespan and Total Strain results for a 6-objects kit.

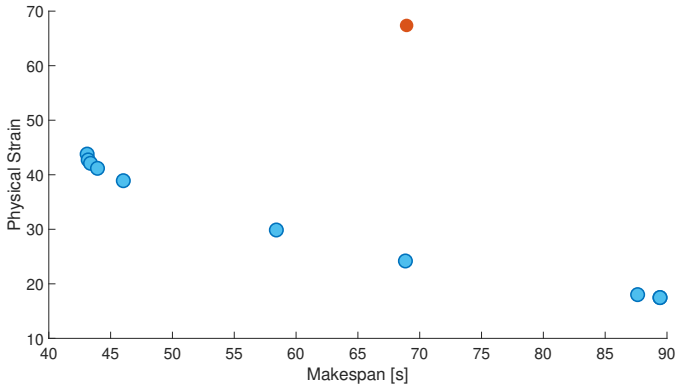

(c) Makespan and Total Strain results for a 9-objects kit.

Figure 5.5: Makespan and Total Strain results for three different kit sizes with random objects. Blue dots are the ones resulting from human-robot collaboration varying α while the red dot represents the baseline, i.e the human worker performs the kit alone.

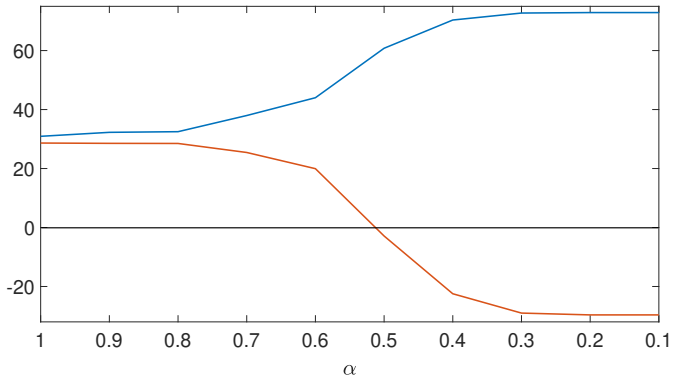

(a) Makespan and Total Strain percentage improvement for a 3-objects kit.

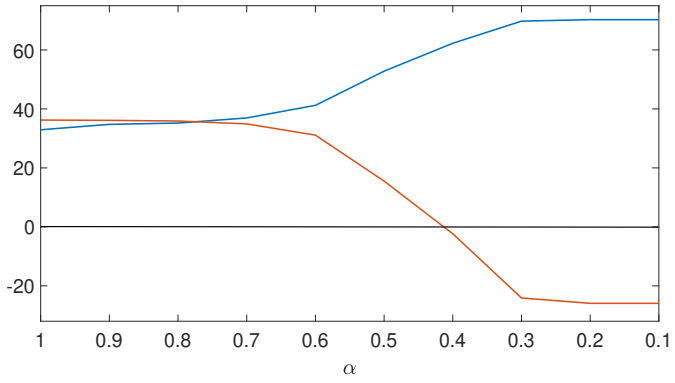

(b) Makespan and Total Strain percentage improvement for a 6-objects kit.

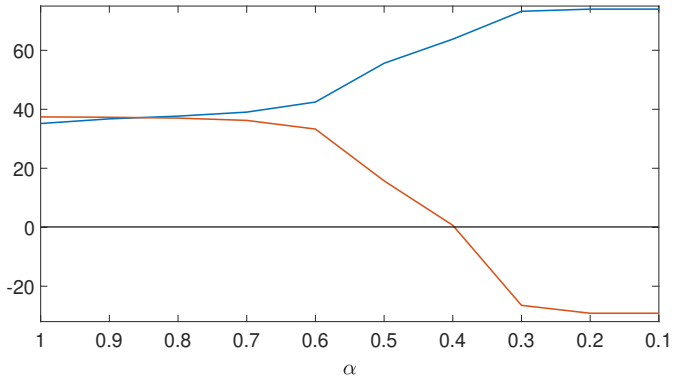

(c) Makespan and Total Strain percentage improvement for a 9-objects kit.

Figure 5.6: Makespan and Total Strain percentage improvement for three different kit sizes with random objects. Blue line represents the total strain improvement while the red one the makespan improvement.

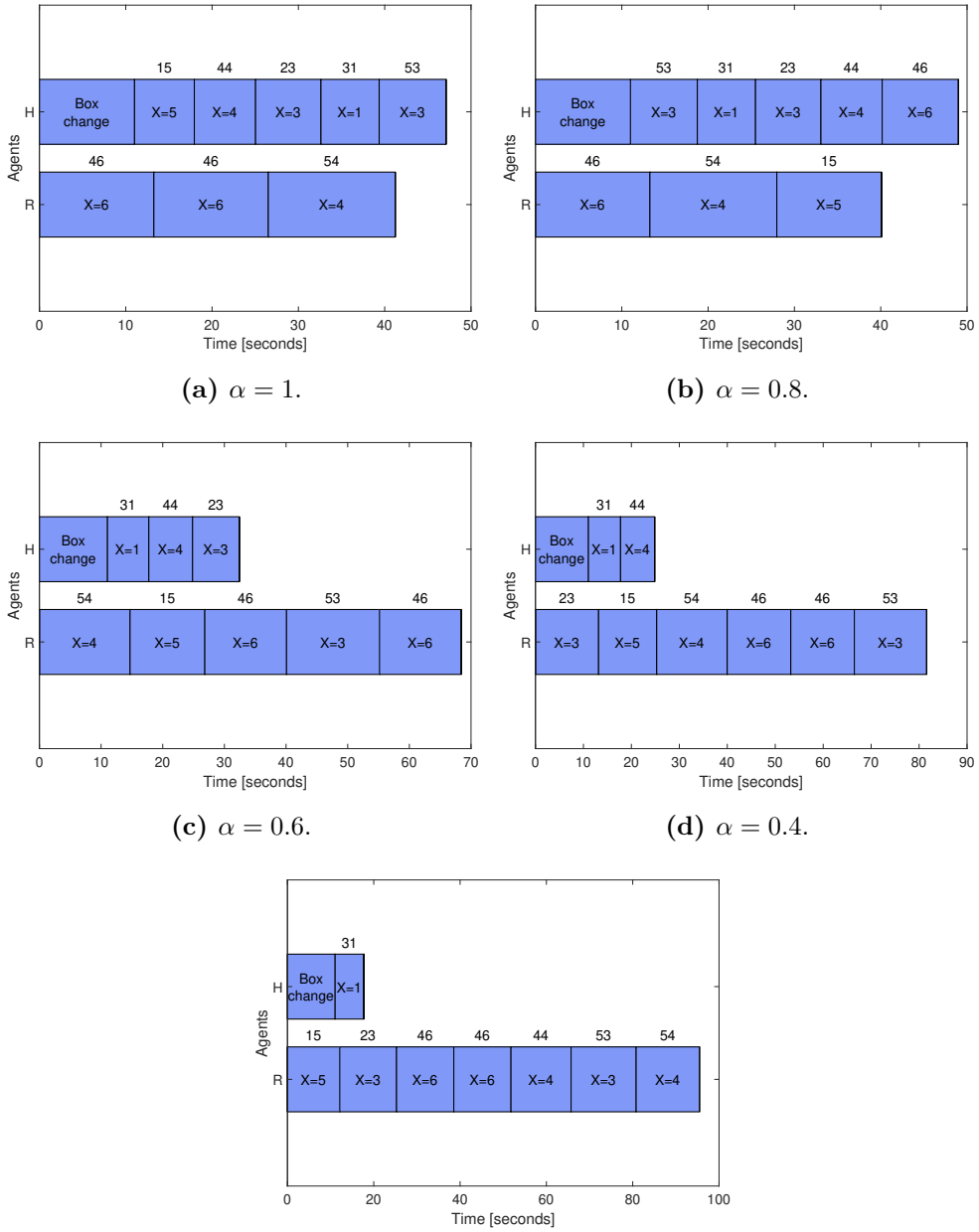

(a) $\alpha = 1$.

(b) $\alpha = 0.8$.

(c) $\alpha = 0.6$.

(d) $\alpha = 0.4$.

(e) $\alpha = 0.3$.

Figure 5.7: Picking action allocations and schedules for human worker and robot under different values of α. Over each picking action duration, the number of the object picked is reported while in the center the object rack position is reported.

(a) (b) (c) (d) (e) (f) (g)

Figure 5.8: Screenshots from a video of the experiment.

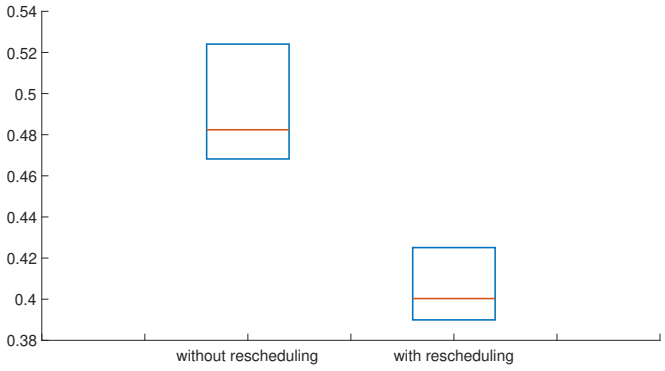

(a) Cost Δ weighted boxplot in the two scheduling approaches.

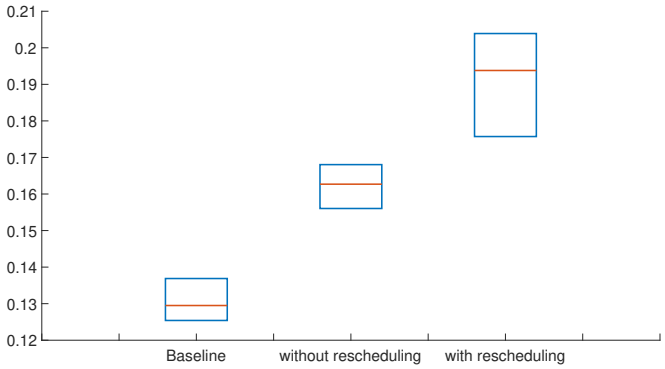

(b) Productivity Λ boxplot in the two scheduling approach and the baseline case.

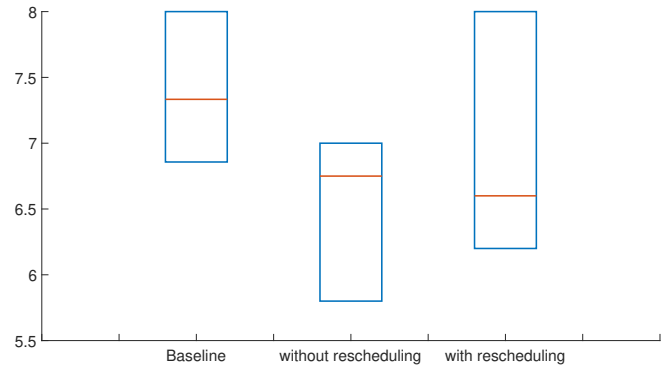

(c) Strain E weighted boxplot in the two scheduling approach and the baseline case.

Figure 5.9: Weighted boxplot of Cost Δ, Productivity Λ and Strain E.

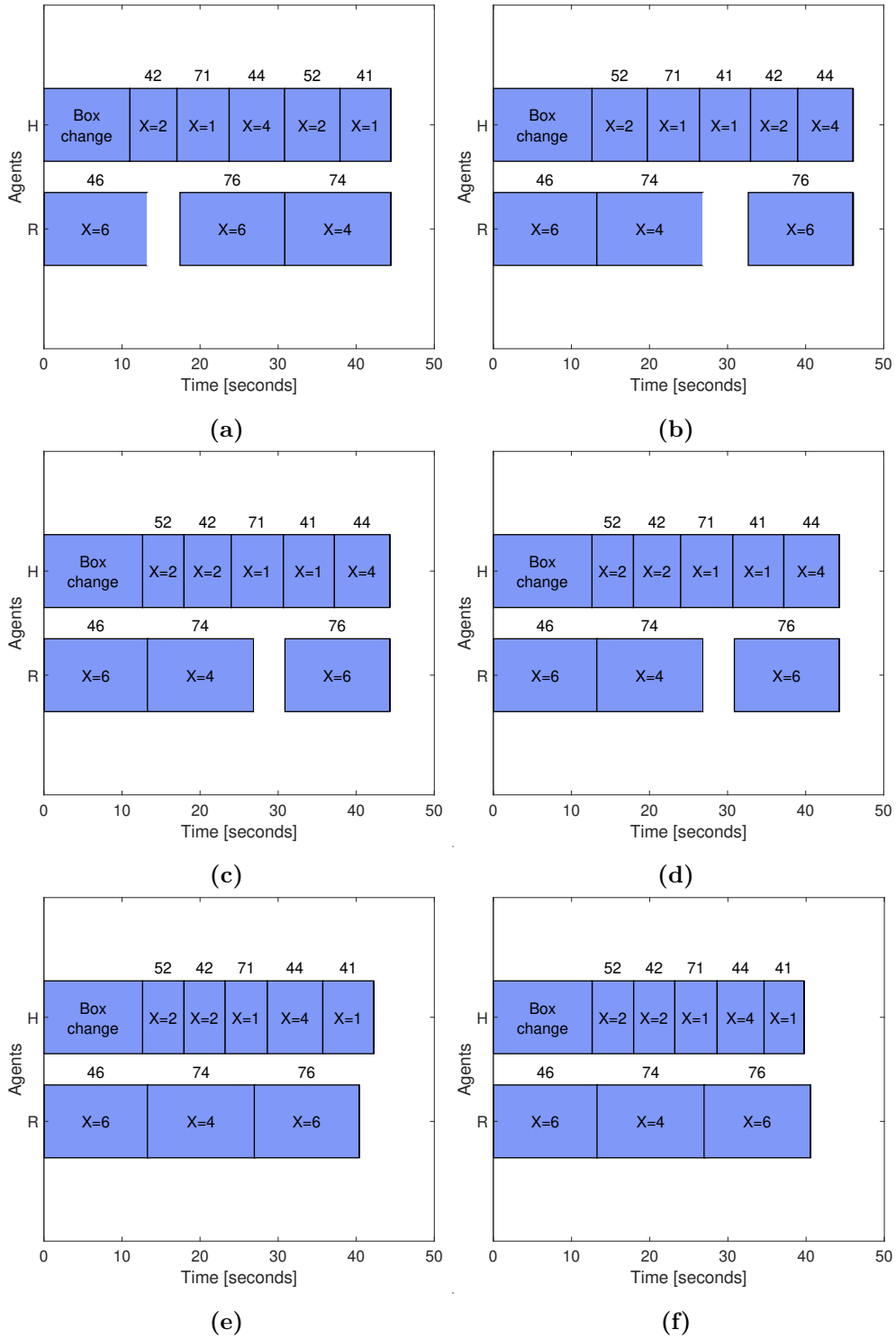

Figure 5.10: Example of the first schedule of the kit (a) and the ones returned by the online reschedule during the cooperative kitting process. Over each picking action duration, the number of the object picked is reported while in the center the object rack position is reported.

Chapter 6

Conclusions and future work

This chapter summarizes the results achieved in this thesis and suggests possible future developments. The aim of the present work was to improve the collaboration between human and robot in kitting operations. The proposed solution relies on an online scheduling algorithm based on the process status generates schedule assigning objects among the two agents improving both the makespan and ergonomics of the process. Afterward, the scheduling algorithm has been implemented on a realistic kitting system in order to validate the algorithm and check performance. Ergonomic information is retrieved from an ergonomic function developed with the REBA method together with Microsoft Kinect. Experimental results show that the online algorithm is able to significantly increase the productivity of the process while reducing the physical strain upon the human worker with respect to both the human-only solution and the offline approach.

A natural extension of this work is the introduction of a human task real-time monitoring. In order to do so, a human completion time estimator must be developed that sends this information to the scheduling algorithm. In fact, in this thesis the human remaining time was always supposed to be zero when the robot rescheduling takes place, that is when the robot cannot pick the next objects because the human is late and it will cause a cross between the two agents. A human completion time estimator would make

it possible to reschedule at any time with a likely increase in performance.

Another possible extension to the present work is to develop an operator's location monitoring system. In this work the collaboration safety was addressed in a simple way, assuming that, the human worker works well, i.e. he takes the right objects and does not invade the work area of the robot during the kitting operation. To address safe human-robot kitting collaboration more in detail the location of the human worker must be continuously monitored and fast arm trajectory replanning considering previously unforeseen obstacles must be realized. [19] already pays attention to this problem and gives suggestions on how to proceed.

Appendix A

REBA Calculation

The REBA method [13], introduced in Chapter 3 provides a posture score that represents the risk of WMSDs from joint angle values. There are two groups, A and B, for the body segments. Calculations of the individual joints composing group A are illustrated in Fig. A.1, A.2, and A.3 while for group B they are illustrated in Fig. A.4, A.5, and A.6. Correspondence Table A.1 and Table A.2 provide the scores for group A (Score A) and B (Score B), respectively. To Score A, obtained from Tab. A.1, we need to add the payload score $\delta_{payload}$:

$$\begin{aligned} if\ load \leq 5\ kg: &\quad \delta_{payload} = 0 \\ if\ load\ between\ 5\ to\ 10\ kg: &\quad \delta_{payload} = 1 \\ if\ load > 10\ kg: &\quad \delta_{payload} = 2 \end{aligned}$$

where *load* corresponds to the weight of the carried object. Finally, the REBA score is obtained from Tab. A.3.

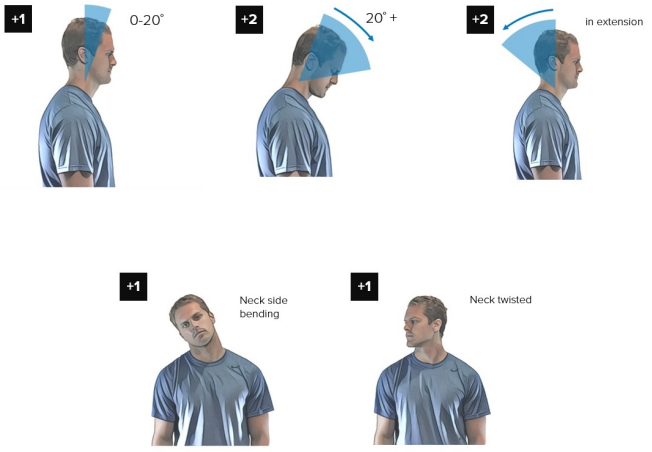

Figure A.1: Group A: Neck position score

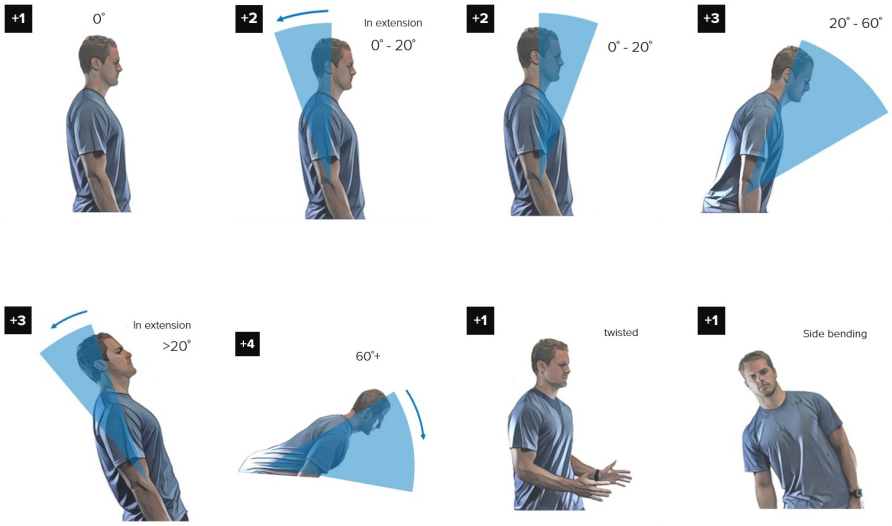

Figure A.2: Group A: Trunk position score

Figure A.3: Group A: Legs position score

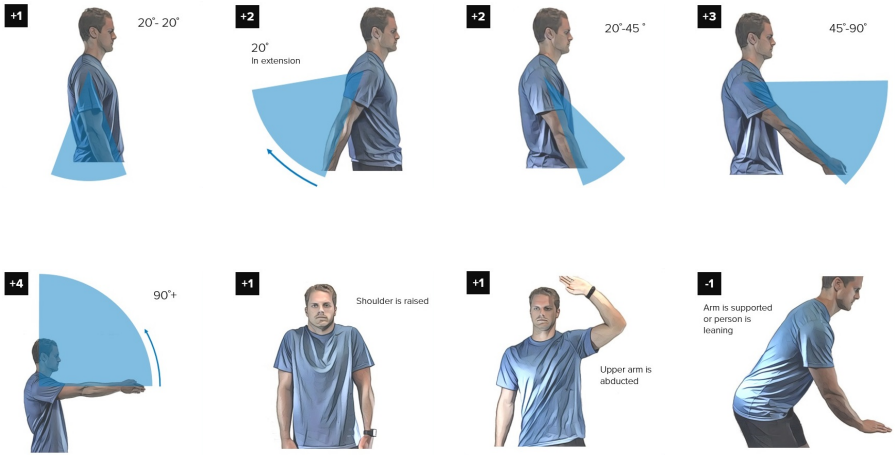

Figure A.4: Group B: Upper arm position score

Figure A.5: Group B: Lower arm position score

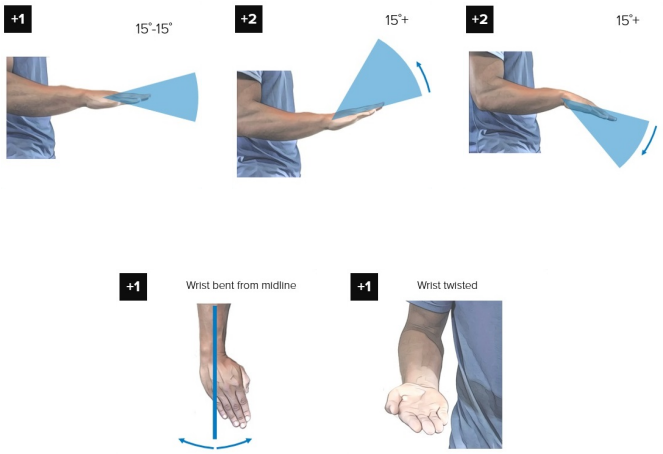

Figure A.6: Group B: Wrist position score

Table A		Neck											
		1				2				3			
	Legs	1	2	3	4	1	2	3	4	1	2	3	4
Trunk	1	1	2	3	4	1	2	3	4	3	3	5	6
	2	2	3	4	5	3	4	5	6	4	5	6	7
	3	2	4	5	6	4	5	6	7	5	6	7	8
	4	3	5	6	7	5	6	7	8	6	7	8	9
	5	4	6	7	8	6	7	8	9	7	8	9	9

Table A.1: Correspondence table for the group A

Table B		Lower Arm					
		1			2		
	Wrist						
		1	2	3	1	2	3
Upper Arm	1	1	2	3	1	2	3
	2	1	2	3	2	3	4
	3	3	4	5	4	5	5
	4	4	5	5	5	6	7
	5	6	7	8	7	8	8
	6	7	8	8	8	9	9

Table A.2: Correspondence table for the group B

Score A	Table C											
	Score B											
	1	2	3	4	5	6	7	8	9	10	11	12
1	1	1	1	2	3	3	4	5	6	7	7	7
2	1	2	2	3	4	4	5	6	6	7	7	8
3	2	3	3	3	4	5	6	7	7	8	8	8
4	3	4	4	4	5	6	7	8	8	9	9	9
5	4	4	4	5	6	7	8	8	9	9	9	9
6	6	6	6	7	8	8	9	9	10	10	10	10
7	7	7	7	8	9	9	9	10	10	11	11	11
8	8	8	8	9	10	10	10	10	10	11	11	11
9	9	9	9	10	10	10	11	11	11	12	12	12
10	10	10	10	11	11	11	11	12	12	12	12	12
11	11	11	11	11	12	12	12	12	12	12	12	12
12	12	12	12	12	12	12	12	12	12	12	12	12

Table A.3: Correspondence table for the REBA score

Bibliography

[1] Cecilia Berlin and Caroline Adams. *Production Ergonomics*. Ubiquity Press, London, Jun 2017.

[2] Mohamed El Amine Boudella, Evren Sahin, and Yves Dallery. Kitting optimisation in just-in-time mixed-model assembly lines: assigning parts to pickers in a hybrid robot–operator kitting system. *International Journal of Production Research*, 56(16):5475–5494, 2018.

[3] Der-San Chen, Robert G Batson, and Yu Dang. *Applied integer programming*. John Wiley and Sons, 2010.

[4] M. Christmansson, L. Medbo, G.-Å. Hansson, K. Ohlsson, J. Unge Byström, T. Möller, and M. Forsman. A case study of a principally new way of materials kitting—an evaluation of time consumption and physical workload. *International Journal of Industrial Ergonomics*, 30(1):49 – 65, 2002.

[5] Comau. Rivalta, 30, 10095 grugliasco, italia. *Homepage: https://www.comau.com/*.

[6] Matthew Crosby, Ronald P. A. Petrick, César Toscano, Rui Correia Dias, Francesco Rovida, and Volker Krüger. Integrating mission, logistics, and task planning for skills-based robot control in industrial kitting applications. In *PlanSIG*, 2016.

[7] Jose Antonio Diego-Mas and Jorge Alcaide-Marzal. Using kinect^{TM} sensor in observational methods for assessing postures at work. *Applied Ergonomics*, 45(4):976 – 985, 2014.

[8] Eurofond. Sixth european working conditions survey: 2015.

[9] Marco Faber, Sinem Kuz, Alexander Mertens, and Christopher M. Schlick. Model-based evaluation of cooperative assembly processes in human-robot collaboration. In Christopher Schlick and Stefan Trzcieliński, editors, *Advances in Ergonomics of Manufacturing: Managing the Enterprise of the Future*, pages 101–112, Cham, 2016. Springer International Publishing.

[10] Christian Finnsgård and Carl Wänström. Factors impacting manual picking on assembly lines: an experiment in the automotive industry. *International Journal of Production Research*, 51(6):1789–1798, 2013.

[11] M. C. Gombolay, R. J. Wilcox, and J. A. Shah. Fast scheduling of robot teams performing tasks with temporospatial constraints. *IEEE Transactions on Robotics*, 34(1):220–239, Feb 2018.

[12] H. Haggag, M. Hossny, S. Nahavandi, and D. Creighton. Real time ergonomic assessment for assembly operations using kinect. In *2013 UKSim 15th International Conference on Computer Modelling and Simulation*, pages 495–500, April 2013.

[13] Sue Hignett and Lynn McAtamney. Rapid entire body assessment (reba). *Applied Ergonomics*, 31(2):201 – 205, 2000.

[14] Stella Y. Hua and Danny J. Johnson. Research issues on factors influencing the choice of kitting versus line stocking. *International Journal of Production Research*, 48(3):779–800, 2010.

[15] I. A Kapandji. *The physiology of the joints*. Churchill Livingstone, 6 edition, 2007.

[16] V. Krueger, A. Chazoule, M. Crosby, A. Lasnier, M. R. Pedersen, F. Rovida, L. Nalpantidis, R. Petrick, C. Toscano, and G. Veiga. A vertical and cyber–physical integration of cognitive robots in manufacturing. *Proceedings of the IEEE*, 104(5):1114–1127, May 2016.

[17] Vito Modesto Manghisi, Antonio Emmanuele Uva, Michele Fiorentino, Vitoantonio Bevilacqua, Gianpaolo Francesco Trotta, and Giuseppe Monno. Real time rula assessment using kinect v2 sensor. *Applied Ergonomics*, 65:481 – 491, 2017.

[18] Lynn McAtamney and E. Nigel Corlett. Rula: a survey method for the investigation of work-related upper limb disorders. *Applied Ergonomics*, 24(2):91 – 99, 1993.

[19] Dmytro Pavlichenko, Germán Martín García, Seongyong Koo, and Sven Behnke. Kittingbot: A mobile manipulation robot for collaborative kitting in automotive logistics. *CoRR*, abs/1809.05380, 2018.

[20] M. Pearce, B. Mutlu, J. Shah, and R. Radwin. Optimizing makespan and ergonomics in integrating collaborative robots into manufacturing processes. *IEEE Transactions on Automation Science and Engineering*, 15(4):1772–1784, Oct 2018.

[21] Pierre Plantard, Hubert P.H. Shum, Anne-Sophie Le Pierres, and Franck Multon. Validation of an ergonomic assessment method using kinect data in real workplace conditions. *Applied Ergonomics*, 65:562 – 569, 2017.

[22] COMAU Robotics. *C4G OPEN System Software Rel. 3.3x*. COMAU Robotics, December 2012.

[23] COMAU Robotics. *Programming Language Manual System Software Rel. 3.3x*. COMAU Robotics, November 2009.

[24] C.J. Sellers and S.Y. Nof. Performance analysis of robotic kitting systems. *Robotics and Computer-Integrated Manufacturing*, 6(1):15 – 24, 1989.

[25] A. Sundin and L. Medbo. Computer visualization and participatory ergonomics as methods in workplace design. *Human Factors and Ergonomics in Manufacturing & Service Industries*, 13(1):1–17, 2003.

[26] Kinya Tamaki and Shimon Y. Nof. Design method of robot kitting sytem for flexible assemble. *Robotics and Autonomous Systems*, 8:255–273, 12 1991.

[27] Panagiota Tsarouchi, Sotiris Makris, and George Chryssolouris. On a human and dual-arm robot task planning method. *Procedia CIRP*, 57:551 – 555, 2016. Factories of the Future in the digital environment - Proceedings of the 49th CIRP Conference on Manufacturing Systems.

[28] Davide Valeriani. *Development of a software library for programming the Comau Smart Six robot manipulator*. PhD thesis, University of Parma, 2010. Unpublished undergraduate dissertation.